

1   **An antisense RNA capable of modulating the  
2   expression of the tumor suppressor microRNA-34a**  
3

4   **Jason T. Serviss<sup>1\*</sup>, Felix Clemens Richter<sup>1,2</sup>, Jimmy Van Den Eynden,  
5   Nathanael Johansson Andrews<sup>1</sup>, Miranda Houtman, Laura  
6   Schwarzmueller, Per Johnsson, Erik Larsson<sup>3</sup>, Dan Grandér<sup>1</sup>, Katja  
7   Pokrovskaja Tamm<sup>1</sup>**

8  
9   <sup>1</sup> Department of Oncology and Pathology, Karolinska Institutet, Stockholm,  
10   Sweden

11   <sup>2</sup> Kennedy Institute of Rheumatology, University of Oxford, Roosevelt Drive,  
12   Oxford OX3 7FY, UK

13   <sup>3</sup>Department of Medical Biochemistry and Cell Biology, Institute of  
14   Biomedicine, The Sahlgrenska Academy, University of Gothenburg, SE-405  
15   30 Gothenburg, Sweden

16   **\* Correspondence:**

17   Jason T. Serviss, Department of Oncology and Pathology, Karolinska  
18   Institutet, Stockholm, Sweden, SE-17177. [jason.serviss@ki.se](mailto:jason.serviss@ki.se)

22   **Abstract**

23   The microRNA-34a is a well-studied tumor suppressor microRNA (miRNA)  
24   that is a direct down-stream target of TP53 and has roles in multiple pathways  
25   associated with oncogenesis, such as proliferation, cellular growth, and  
26   differentiation. Due to its wide variety of targets that suppress oncogenesis, it  
27   is not surprising that miR34a expression has been shown to be dys-regulated  
28   in a wide variety of both solid tumors and hematological malignancies.  
29   Despite this, the mechanisms by which miR34a is regulated in these cancers  
30   is not well studied. Here we find that the *miR34a* antisense RNA, a long non-  
31   coding RNA transcribed antisense to *miR34a*, is critical  
32   for *miR34a* expression and mediation of its cellular functions in multiple types  
33   of human cancer. In addition, we characterize miR34a asRNA's ability to  
34   facilitate miR34a expression under multiple types of cellular stress in both  
35   TP53 deficient and wild-type settings.

36 **Introduction**

37 In recent years advances in functional genomics has revolutionized our  
38 understanding of the human genome. Evidence now points to the fact that  
39 approximately 75% of the genome is transcribed but only ~1.2% of this is  
40 responsible for encoding proteins (International Human Genome Sequencing  
41 2004, Djebali et al. 2012). Of these recently identified elements, long non-  
42 coding (lnc) RNAs are defined as transcripts exceeding 200bp in length with a  
43 lack of a functional open reading frame. Some lncRNAs are dually classified  
44 as antisense (as) RNAs that are expressed from the same locus as a sense  
45 transcript in the opposite orientation. Current estimates using high-throughput  
46 transcriptome sequencing, indicate that up to 20-40% of the approximately  
47 20,000 protein-coding genes exhibit antisense transcription (Chen et al. 2004,  
48 Katayama et al. 2005, Ozsolak et al. 2010). The hypothesis that asRNAs play  
49 an important role in oncogenesis was first proposed when studies increasingly  
50 found examples of aberrant expression of these transcripts and other lncRNA  
51 subgroups in tumor samples (Balbin et al. 2015). Although studies  
52 characterizing the functional importance of asRNAs in cancer are limited to  
53 date, characterization a number of individual transcripts has led to the  
54 discovery of multiple examples of asRNA-mediated regulation of several well  
55 known tumorigenic factors (Yap et al. 2010, Johnsson et al. 2013). The  
56 mechanisms by which asRNAs accomplish this are diverse, and include  
57 recruitment of chromatin modifying factors (Rinn et al. 2007), acting as  
58 microRNA (miRNA) sponges (Memczak et al. 2013), and causing  
59 transcriptional interference (Conley et al. 2012).

60

61 Responses to cellular stress, e.g. DNA damage, sustained oncogene  
62 expression, and nutrient deprivation, are all tightly monitored and orchestrated  
63 cellular pathways that are commonly dys-regulated in cancer. Cellular  
64 signaling in response to these types of cellular stress often converge on the  
65 transcription factor TP53 that regulates transcription of coding and non-coding  
66 downstream targets. One non-coding target of TP53 is the tumor suppressor  
67 microRNA known as *miR34a* (Raver-Shapira et al. 2007).  
68 Upon TP53 activation *miR34a* expression is increased allowing it to down-  
69 regulate its targets involved in cellular pathways such as, growth factor  
70 signaling, apoptosis, differentiation, and cellular senescence (Lal et al. 2011,  
71 Slabakova et al. 2017). *miR34a* is a crucial factor in mediating activated TP53  
72 response and it is often deleted or down-regulated in human cancers and has  
73 also been shown to be a valuable prognostic marker (Cole et al. 2008,  
74 Gallardo et al. 2009, Zenz et al. 2009, Cheng et al. 2010, Liu et al. 2011).  
75 Reduced *miR34a* transcription is mediated via epigenetic regulation in many  
76 solid tumors, such as colorectal-, pancreatic-, and ovarian cancer (Vogt et al.  
77 2011), as well as multiple types of hematological malignancies (Chim et al.  
78 2010). In addition, miR34a has been shown to be transcriptionally regulated  
79 via TP53 homologs, TP63 and TP73, other transcription factors, e.g. STAT3  
80 and MYC, and, in addition, post-transcriptionally through miRNA sponging by  
81 the NEAT1 lncRNA (Chang et al. 2008, Su et al. 2010, Agostini et al. 2011,  
82 Rokavec et al. 2015, Ding et al. 2017). Despite these findings, the  
83 mechanisms underlying miR34a regulation in the context of oncogenesis have  
84 not yet been fully elucidated.

85

86 Studies across multiple cancer types have reported a decrease in oncogenic  
87 phenotypes when miR34a expression is induced in a p53-null background,  
88 although endogenous mechanisms for achieving this have not yet been  
89 discovered (Liu et al. 2011, Ahn et al. 2012, Yang et al. 2012, Stahlhut et al.  
90 2015, Wang et al. 2015). In addition, previous reports have identified a  
91 lncRNA originating in the antisense orientation from the miR34a locus which  
92 is regulated by TP53 and is induced upon multiple forms of cellular stress  
93 (Rashi-Elkeles et al. 2014, Hunten et al. 2015, Leveille et al. 2015, Ashouri et  
94 al. 2016, Kim et al. 2017). Despite this, none of these studies have continued  
95 to functionally characterize this transcript. In this study we functionally  
96 characterize the *miR34a* asRNA transcript, and find that modulating the levels  
97 of the *miR34a* asRNA is sufficient to increase levels of *miR34a* and results in  
98 a decrease of multiple tumorigenic phenotypes. Furthermore, we find that  
99 *miR34a* asRNA-mediated up-regulation of *miR34a* is sufficient to induce  
100 endogenous cellular mechanisms counteracting several types of stress stimuli  
101 in a *TP53* deficient background. Finally, similar to the functional roles of  
102 antisense transcription at protein-coding genes, we identify an example of an  
103 antisense RNA capable of regulating a cancer-associated miRNA.

104

## 105 **Results**

106

107 ***miR34a* asRNA is a broadly expressed, non-coding transcript whose**  
108 **levels correlate with *miR34a* expression**

109

110 *miR34a* asRNA is transcribed in a “head-to-head” orientation with  
111 approximately 100 base pair overlap with the *miR34a* host gene (HG) (**Fig.**  
112 **1a**). Due to the fact that sense/antisense pairs can be both concordantly and  
113 discordantly expressed, we sought to evaluate this relationship in the case of

114 *miR34a* HG and its asRNA. Using a diverse panel of cancer cell lines, we  
115 detected co-expression of both the *miR34a* HG and *miR34a* asRNA (**Fig. 1b**).  
116 We included *TP53*+/+, *TP53* mutated, and *TP53*-/- cell lines in the panel due  
117 to previous reports that *miR34a* is a known downstream target of TP53.  
118 These results indicate that *miR34a* HG and *miR34a* asRNA are co-expressed  
119 and that their expression levels correlate with *TP53* status, with *TP53*-/- cell  
120 lines tending to have decreased or abolished expression of both transcripts.

121

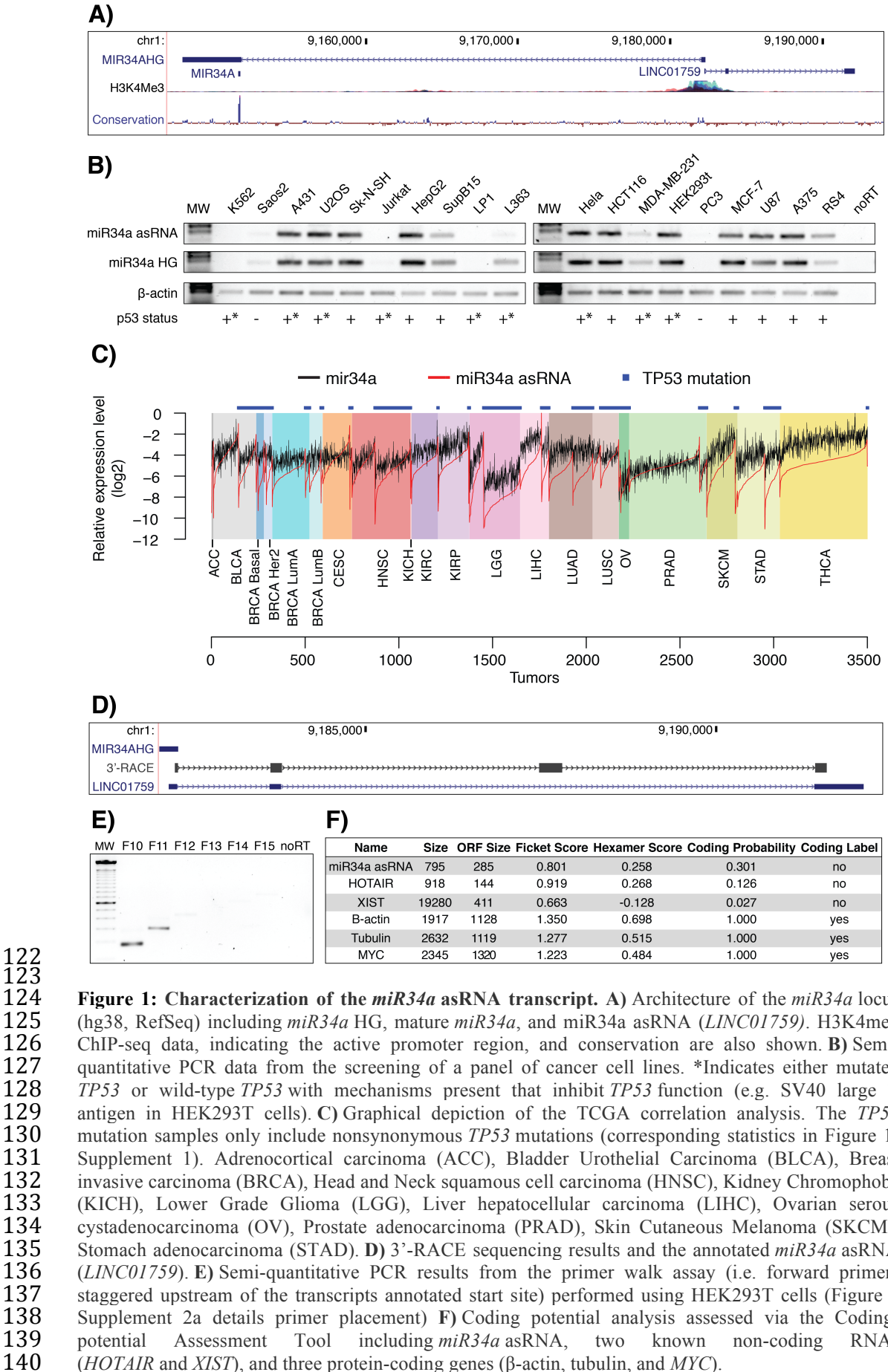


**Figure 1: Characterization of the *miR34a* asRNA transcript.** A) Architecture of the *miR34a* locus (hg38, RefSeq) including *miR34a* HG, mature *miR34a*, and *miR34a* asRNA (*LINC01759*). H3K4me3 ChIP-seq data, indicating the active promoter region, and conservation are also shown. B) Semi-quantitative PCR data from the screening of a panel of cancer cell lines. \*Indicates either mutated *TP53* or wild-type *TP53* with mechanisms present that inhibit *TP53* function (e.g. SV40 large T antigen in HEK293T cells). C) Graphical depiction of the TCGA correlation analysis. The *TP53* mutation samples only include nonsynonymous *TP53* mutations (corresponding statistics in Figure 1-Supplement 1). Adrenocortical carcinoma (ACC), Bladder Urothelial Carcinoma (BLCA), Breast invasive carcinoma (BRCA), Head and Neck squamous cell carcinoma (HNSC), Kidney Chromophobe (KICH), Lower Grade Glioma (LGG), Liver hepatocellular carcinoma (LIHC), Ovarian serous cystadenocarcinoma (OV), Prostate adenocarcinoma (PRAD), Skin Cutaneous Melanoma (SKCM), Stomach adenocarcinoma (STAD). D) 3'-RACE sequencing results and the annotated *miR34a* asRNA (*LINC01759*). E) Semi-quantitative PCR results from the primer walk assay (i.e. forward primers staggered upstream of the transcripts annotated start site) performed using HEK293T cells (Figure 1 Supplement 2a details primer placement) F) Coding potential analysis assessed via the Coding-potential Assessment Tool including *miR34a* asRNA, two known non-coding RNAs (*HOTAIR* and *XIST*), and three protein-coding genes ( $\beta$ -actin, tubulin, and *MYC*).

141 We next sought to interrogate primary cancer samples to examine if a  
142 correlation between *miR34a* asRNA and *miR34a* expression levels could be  
143 identified. For this task we utilized RNA sequencing data from The Cancer  
144 Genome Atlas (TCGA) after stratifying patients by cancer type, *TP53* status  
145 and, where appropriate, cancer subtypes. The results indicate  
146 that *miR34a* asRNA and *miR34a* expression are strongly correlated in the  
147 vast majority of cancer types examined, both in the presence and absence of  
148 wild-type *TP53* (**Fig. 1c, Figure 1-Figure Supplement 1a**). The results also  
149 further confirm that the expression levels of both *miR34a* and its asRNA tend  
150 to be reduced in patients with nonsynonymous *TP53* mutations (**Figure 1-**  
151 **Figure Supplement 1b**).

152

153 Next, we aimed to gain a thorough understanding of *miR34a* asRNA's  
154 molecular characteristics and cellular localization. To experimentally  
155 determine the 3' termination site for the *miR34a* asRNA transcript we  
156 performed 3' rapid amplification of cDNA ends (RACE) using the U2OS  
157 osteosarcoma cell line that exhibited high endogenous levels  
158 of *miR34a* asRNA in the cell panel screening. Sequencing the cloned cDNA  
159 indicated that the transcripts 3' transcription termination site is 525 base pairs  
160 upstream of the *LINC01759* transcript's annotated termination site (**Fig. 1d**).  
161 Next, we characterized the *miR34a* asRNA 5' transcription start site by  
162 carrying out a primer walk assay, i.e. a common reverse primer was placed in  
163 exon 2 and forward primers were gradually staggered upstream of the  
164 transcripts annotated start site (**Figure 1-Figure Supplement 2a**). Our results  
165 indicated that the 5' start site for *miR34a* asRNA is in fact approximately 90bp

166 (F11 primer) to 220bp (F12 primer) upstream of the annotated start site (**Fig.**  
167 **1e**). Polyadenylation status was evaluated via cDNA synthesis with either  
168 random nanomers or oligoDT primers followed by semi-quantitative PCR with  
169 results indicating that the *miR34a* asRNA is polyadenylated although the  
170 unspliced form seems to only be in the polyA negative state (**Figure 1-Figure**  
171 **Supplement 2b**). We furthermore investigated the propensity  
172 of *miR34a* asRNA to be alternatively spliced in U2OS cells, using PCR  
173 cloning and sequencing and found that the transcript is post-transcriptionally  
174 spliced to form multiple different isoforms (**Figure 1-Figure Supplement 2c**).  
175 Finally, to evaluate the cellular localization of *miR34a* asRNA we utilized RNA  
176 sequencing data from five cancer cell lines included in the ENCODE  
177 (Consortium 2012) project that had been fractionated into cytosolic and  
178 nuclear fractions. The analysis revealed that the *miR34a* asRNA transcript  
179 localizes to both the nucleus and cytoplasm but primarily resides in the  
180 nucleus (**Figure 1-Figure Supplement 2d**).

181

182 Finally, we utilized multiple approaches to evaluate the coding potential of  
183 the *miR34a* asRNA transcript. The Coding-Potential Assessment Tool is a  
184 bioinformatics-based tool that uses a logistic regression model to evaluate  
185 coding-potential by examining ORF length, ORF coverage, Fickett score and  
186 hexamer score (Wang et al. 2013). Results indicated that *miR34a* asRNA has  
187 a similar lack of coding capacity to the known non-coding  
188 transcripts *HOTAIR* and *XIST* and differs greatly when examining these  
189 parameters to the known coding transcripts  $\beta$ -actin, tubulin, and *MYC* (**Fig.**  
190 **1F**). We further confirmed these results using the Coding-Potential Calculator

191 that utilizes a support based machine-based classifier and accesses an  
192 alternate set of discriminatory features (**Figure 1-Figure Supplement 2e**)  
193 (Kong et al. 2007). \*\*\* We hope to be able to scan for peptides matching to  
194 miR34a asRNA in CPTAC and Geiger et al., 2012 before submission and will  
195 mention results here.\*\*\*

196

### 197 **TP53-mediated regulation of *miR34a* asRNA expression**

198 *miR34a* is a known downstream target of TP53 and has been previously  
199 shown to exhibit increased expression within multiple contexts of cellular  
200 stress. *miR34a* asRNA has also been shown to be induced upon TP53  
201 activation in several global analyses of p53-regulated lncRNAs (Rashi-Elkeles  
202 et al. 2014, Hunten et al. 2015, Leveille et al. 2015, Ashouri et al. 2016, Kim et  
203 al. 2017). To confirm these results in our biological system, we treated  
204 HEK293t, embryonic kidney cells, and HCT116, colorectal cancer cells, with  
205 the DNA damaging agent doxorubicin to activate TP53. QPCR-mediated  
206 measurement of both *miR34a* HG and asRNA indicated that their expression  
207 levels were increased in response to doxorubicin treatment in both cell lines  
208 (**Fig. 2a**). To assess if it is in fact *TP53* that is responsible for the increase  
209 in *miR34a* asRNA expression upon DNA damage, we  
210 treated *TP53*<sup>+/+</sup> and *TP53*<sup>-/-</sup> HCT116 cells with increasing concentrations of  
211 doxorubicin and monitored the expression of both *miR34a* HG and asRNA.  
212 We observed a dose-dependent increase in both *miR34a* HG and asRNA  
213 expression levels with increasing amounts of doxorubicin, indicating that  
214 these two transcripts are co-regulated, although, this effect was largely  
215 abrogated in *TP53*<sup>-/-</sup> cells (**Fig. 2b**). These results indicate

216 that *TP53* activation increases *miR34a* asRNA expression upon the induction  
217 of DNA damage. Nevertheless, *TP53*<sup>-/-</sup> cells also showed a dose dependent  
218 increase in both *miR34a* HG and asRNA, indicating that additional factors,  
219 other than *TP53*, are capable of initiating an increase in expression of both of  
220 these transcripts upon DNA damage.

221

222  
223  
224  
225  
226  
227  
228  
229  
230  
231  
232  
233  
234  
235  
236

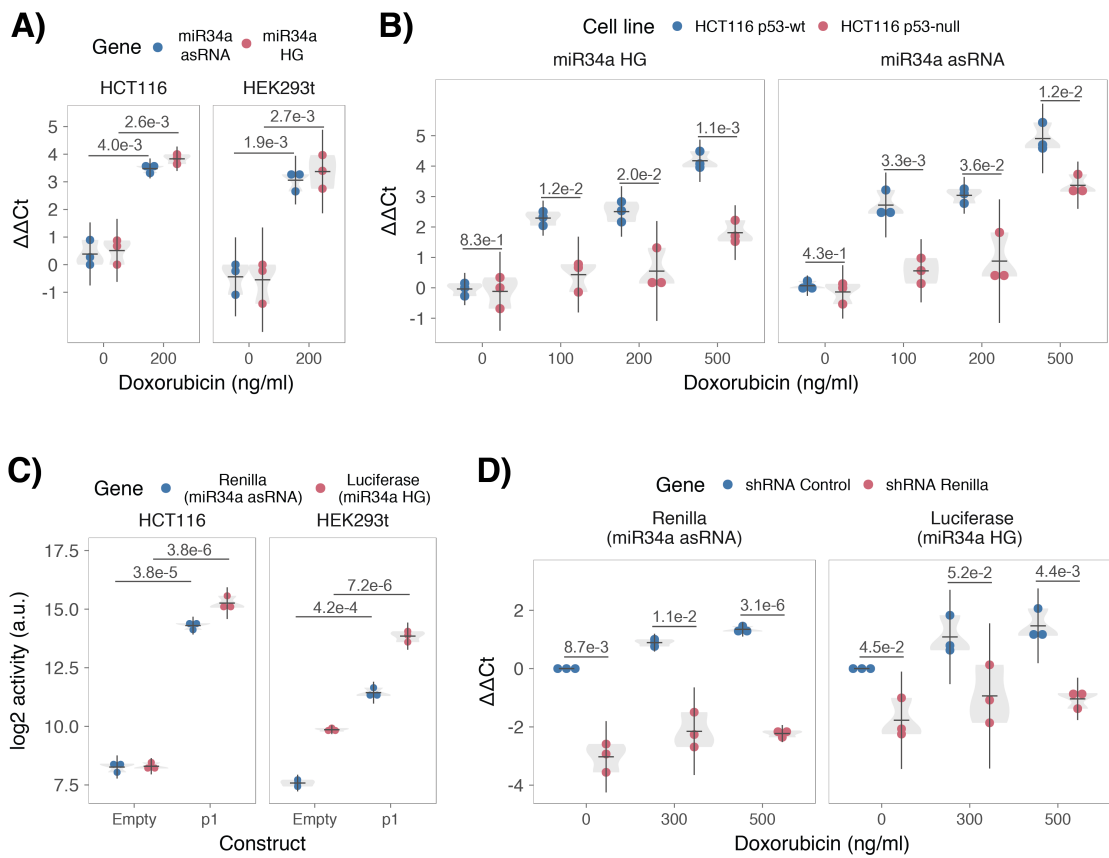


**Figure 2: TP53-mediated regulation of the *miR34a* locus.** **A)** Evaluating the effects of 24 hours of treatment with 200 ng/ml doxorubicin on *miR34a* asRNA and HG in HCT116 and HEK293t cells.\* **B)** Monitoring *miR34a* HG and asRNA expression levels during 24 hours doxorubicin treatment in *TP53*<sup>+/+</sup> and *TP53*<sup>-/-</sup> HCT116 cells.\* **C)** Quantification of luciferase and renilla levels after transfection of HCT116 and HEK293T cells with the p1 construct (Figure 2 Supplement 2 contains a schematic representation of the p1 construct).\* **D)** HCT116 cells were co-transfected with the p1 construct and shRNA renilla or shRNA control and subsequently treated with increasing doses of doxorubicin. 24 hours post-treatment, cells were harvested and renilla and luciferase levels were measured using QPCR. Resulting p-values from statistical testing are shown above the shRenilla samples which were compared to the shRNA control using the respective treatment condition.\* Individual points represent results from independent experiments and the gray shadow indicates the density of those points. Error bars show the 95% CI, black horizontal lines represent the mean, and p-values are shown over long horizontal lines indicating the comparison tested.

237 The head-to head orientation of *miR34a* HG and asRNA, suggests that  
238 transcription is initiated from a single promoter in a bi-directional manner. To  
239 investigate whether *miR34a* HG and asRNA are transcribed from the same  
240 promoter as divergent transcripts, we cloned the *miR34a* HG promoter,  
241 including the *TP53* binding site, into a luciferase/renilla dual reporter vector  
242 which we hereafter refer to as p1 (**Figure 2-Figure Supplement 1a-b**). Upon  
243 transfection of p1 into HCT116 and HEK293t cell lines we observed increases  
244 in both luciferase and renilla indicating that *miR34a* HG and asRNA  
245 expression can be regulated by a single promoter contained within the p1  
246 construct (**Fig. 2c**).

247

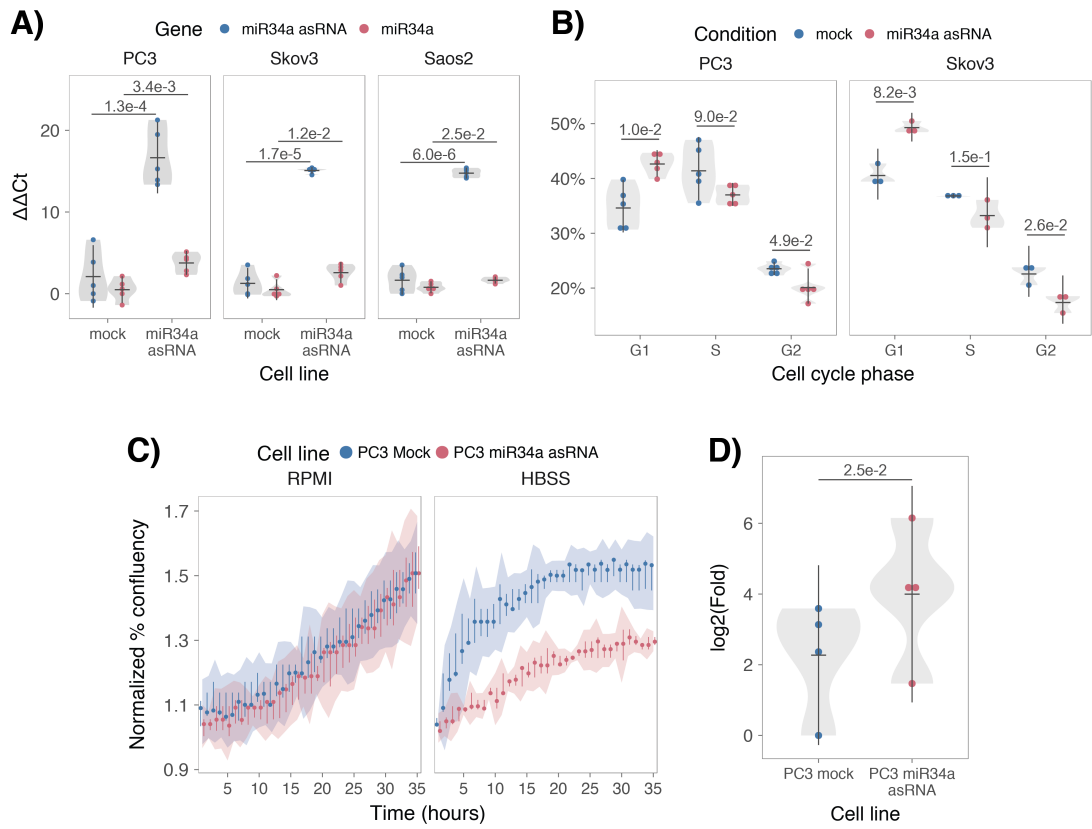
248 We hypothesized that *miR34a* asRNA may regulate *miR34a* HG levels and, in  
249 addition, that the overlapping regions of the sense and antisense transcripts  
250 may have a crucial role in mediating this regulation. Knock-down of  
251 endogenous *miR34a* asRNA is complicated by its various isoforms (**Figure 1-**  
252 **Figure Supplement 2c**). For this reason, we utilized the p1 construct to  
253 evaluate the regulatory role of the miR34a asRNA on miR34a HG.  
254 Accordingly, we first co-transfected the p1 construct, containing the  
255 overlapping region of the two transcripts, and two different short hairpin (sh)  
256 RNAs targeting renilla into HEK293T cells and subsequently measured  
257 luciferase and renilla expression. The results indicated that shRNA-mediated  
258 knock down of the p1-renilla transcript (corresponding to *miR34a* asRNA)  
259 caused p1-luciferase (corresponding to *miR34a* HG) levels to concomitantly  
260 decrease (**Figure 2-Figure Supplement 2**). These results indicate  
261 that *miR34a* asRNA positively regulates levels of *miR34a* HG and that the

262 transcriptional product of the *miR34a* asRNA within in the p1 construct  
263 promotes a miR34a response. To further support these conclusions and  
264 better understand the role of miR34a asRNA during TP53 activation, *TP53*<sup>+/+</sup>  
265 HCT116 cells were co-transfected with p1 and shRNA renilla (2.1) and  
266 subsequently treated with increasing doses of doxorubicin. Again, the results  
267 showed a concomitant reduction in luciferase levels upon knock-down of p1-  
268 renilla i.e. the *miR34a* asRNA corresponding segment of the p1 transcript  
269 (**Fig. 2d**). Furthermore, the results showed that in the absence of p1-renilla  
270 the expected induction of p1-luciferase in response to TP53 activation to DNA  
271 damage is abrogated. Collectively these results indicate that *miR34a* asRNA  
272 positively regulates *miR34a* expression and is crucial for an appropriate  
273 TP53-mediated *miR34a* response to DNA damage.

274

275 ***miR34a* asRNA regulates its host gene independently of *TP53***  
276 Despite the fact that TP53 regulates *miR34a* HG and asRNA expression, our  
277 results indicated that other factors are also able to regulate this locus (**Fig.**  
278 **2b**). Utilizing a lentiviral system, we stably over-expressed the *miR34a* asRNA  
279 transcript in three *TP53*-null cell lines, PC3 (prostate cancer), Saos2  
280 (osteogenic sarcoma), and Skov3 (adenocarcinoma). We first analyzed the  
281 levels of *miR34a* asRNA in these stable over-expression cell lines, compared  
282 to HEK293T cells, which have high endogenous levels of *miR34a* asRNA,  
283 finding that, on average, the over-expression was approximately 30-fold  
284 higher in the over-expression cell lines than in HEK293t cells. Due to the fact  
285 that *miR34a* asRNA can be up-regulated ~30-fold in response to DNA  
286 damage (**Fig. 2b**), we deemed this over-expression level to correspond to

287 physiologically relevant levels in cells encountering a stress stimulus, such as  
288 DNA damage (**Figure 3-Figure Supplement 1**). Analysis of *miR34a* levels in  
289 the *miR34a* asRNA over-expressing cell lines showed that this over-  
290 expression resulted in a concomitant increase in the expression of *miR34a* in  
291 all three cell lines (**Fig. 3a**). These results indicate that, in the absence of  
292 *TP53*, *miR34a* expression may be rescued by increasing the levels  
293 of *miR34a* asRNA expression.



294

295 **Figure 3: miR34a asRNA positively regulates miR34a and its associated phenotypes.** A) QPCR-  
296 mediated quantification of miR34a expression in cell lines stably over-  
297 expressing miR34a asRNA.\* B) Cell cycle analysis comparing stably over-expressing miR34a asRNA  
298 cells to the respective mock expressing cells.\* C) Analysis of cellular growth over time in miR34a  
299 asRNA over-expressing PC3 cells. Points represent the median from 3 independent experiments, the  
300 colored shadows indicate the 95% confidence interval, and vertical lines show the minimum and  
301 maximum values obtained from the three biological replicates. D) Differential phosphorylated  
302 polymerase II binding in miR34a asRNA over-expressing PC3 cells.\* \*Individual points represent  
303 results from independent experiments and the gray shadow indicates the density of those points. Error  
304 bars show the 95% CI, black horizontal lines represent the mean, and p-values are shown over long  
305 horizontal lines indicating the comparison tested.  
306

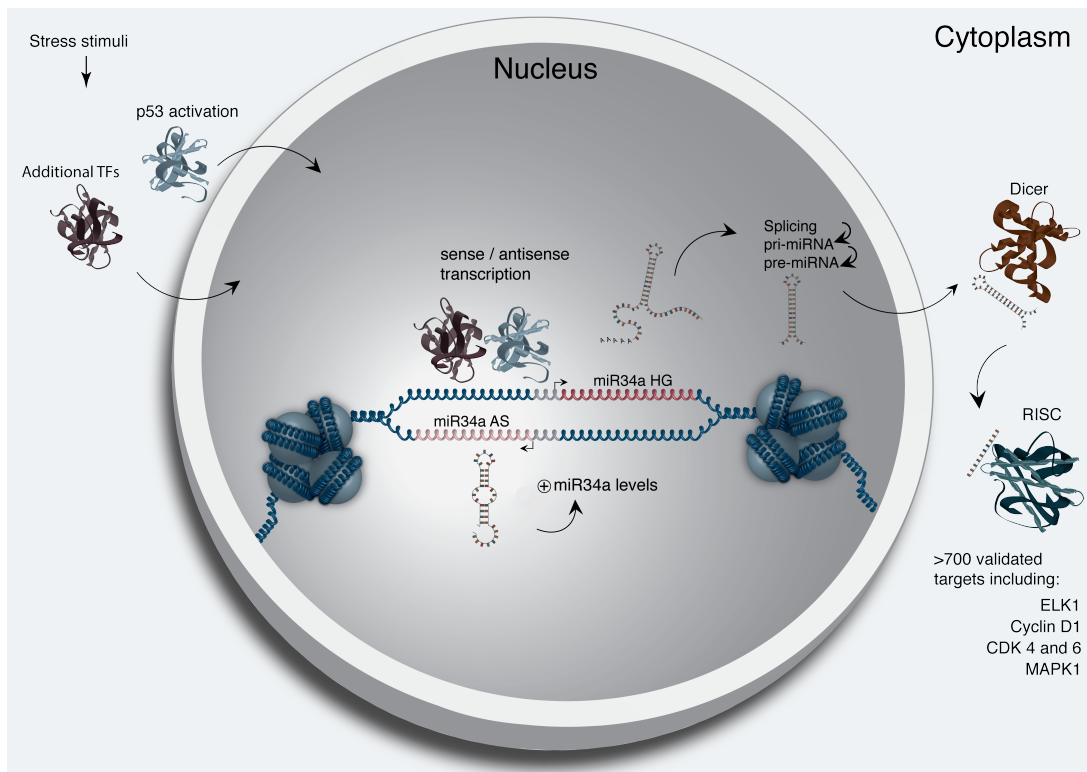
307 *miR34a* has been previously shown to regulate cell cycle progression, with  
308 *miR34a* induction causing G1 arrest (Raver-Shapira et al. 2007, Tarasov et al.  
309 2007). Cell cycle analysis via determination of DNA content showed a  
310 significant increase in G1 phase cells in the PC3 and Skov3 *miR34a* asRNA  
311 over-expressing cell lines, indicative of G1 arrest, as well as, a significant  
312 decrease of cells in G2 phase (**Fig. 3b**). *miR34a*'s effects on the cell cycle are  
313 mediated by its ability to target cell cycle regulators such as cyclin D1  
314 (*CCND1*) (Sun et al. 2008). We therefore sought to determine if  
315 the *miR34a* asRNA over-expressing cell lines exhibited effects on this  
316 known *miR34a* target. Quantification of both *CCND1* RNA expression (**Figure**  
317 **3-Figure Supplement 2a**) and protein levels (**Figure 3-Figure Supplement**  
318 **2b**) in the PC3 *miR34a* asRNA over-expressing cell line showed a significant  
319 decrease of *CCND1* levels compared to the mock control.

320  
321 *miR34a* is also a well known inhibitor of cellular growth via its ability to  
322 negatively regulate growth factor signaling. Furthermore, starvation has been  
323 shown to induce *miR34a* expression that down-regulates multiple targets that  
324 aid in the phosphorylation of pro-survival growth factors (Lal et al. 2011). We  
325 further interrogated the effects of *miR34a* asRNA over-expression by  
326 monitoring the growth of the cells in both normal and starvation conditions via  
327 confluency measurements over a 35-hour period. Under normal growth  
328 conditions there is a small but significant reduction ( $p = 3.0\text{e-}8$ ) in confluency  
329 in the *miR34a* asRNA over-expressing cell lines although, these effects on  
330 cell growth are drastically increased in starvation conditions ( $p = 9.5\text{e-}67$ ).  
331 This is in accordance with our previous results, and suggests

332 that *miR34a* asRNA-mediated increases in *miR34a* expression are crucial  
333 under conditions of stress and necessary for the initiation of an appropriate  
334 cellular response. In summary, we find that over-expression  
335 of *miR34a* asRNA is sufficient to increase *miR34a* expression and gives rise  
336 to known phenotypes observed with induction of *miR34a*.

337

338 Antisense RNAs have been reported to mediate their effects both via  
339 transcriptional and post-transcriptional mechanisms. Due to the fact that  
340 *miR34a* expression is undetected in wild type PC3 cells but, upon over-  
341 expression of *miR34a* asRNA, increases to detectable levels, we  
342 hypothesized that *miR34a* asRNA is capable of regulating *miR34a* expression  
343 via a transcriptional mechanism. To ascertain if this is actually the case, we  
344 performed chromatin immunoprecipitation (ChIP) for phosphorylated  
345 polymerase II (polII) at the *miR34a* HG promoter in both *miR34a* asRNA over-  
346 expressing and mock control cell lines. Our results indicated a clear increase  
347 in phosphorylated polII binding at the *miR34a* promoter upon *miR34a* asRNA  
348 over-expression indicating the ability of *miR34a* asRNA to regulate *miR34a*  
349 levels on a transcriptional level (**Fig. 3d**).



350

351 **Figure 4: A graphical summary of the proposed *miR34a* asRNA function.** Stress stimuli,  
352 originating in the cytoplasm or nucleus, activates *TP53* as well as additional factors. These factors then  
353 bind to the *miR34a* promoter and drive transcription of the sense and antisense strands. *miR34a* asRNA  
354 serves to increase the levels of *miR34a* HG transcription via an unknown mechanism. *miR34a* HG  
355 then, in turn, is then spliced, processed by the RNase III enzyme Drosha, and exported to the  
356 cytoplasm. The *miR34a* pre-miRNA then binds to Dicer where the hair-pin loop is cleaved and  
357 mature *miR34a* is formed. Binding of the mature *miR34a* miRNA to the RISC complex then allows it  
358 to bind and repress its targets.

359 **Discussion**

360  
361 Multiple studies have previously shown asRNAs to be crucial for the  
362 appropriate regulation of cancer-associated protein-coding genes and that  
363 their dys-regulation can lead to perturbation of tumor suppressive and  
364 oncogenic pathways, as well as, cancer-related phenotypes (Yu et al. 2008,  
365 Yap et al. 2010, Serviss et al. 2014, Balbin et al. 2015). Here we show that  
366 asRNAs are also capable of regulating cancer-associated miRNAs resulting in  
367 similar consequences as protein-coding gene dys-regulation (**Fig. 4**).  
368 Interestingly, we show that, both in the presence and absence of  
369 *TP53*, *miR34a* asRNA provides an additional regulatory level and functions by  
370 mediating the increase of *miR34a* expression in both homeostasis and upon  
371 encountering multiple forms of cellular stress. Furthermore, we find that  
372 *miR34a* asRNA-mediated increases in *miR34a* expression levels are sufficient  
373 to drive the appropriate cellular responses to multiple forms of stress stimuli  
374 that are encountered (**Fig. 2d and Fig. 3c**). Previous studies have utilized  
375 various molecular methods to up regulate *miR34a* expression in a p53  
376 deficient background showing similar phenotypic outcomes but, to our  
377 knowledge, this is the first example of an endogenous mechanism by which  
378 this can be achieved (Liu et al. 2011, Ahn et al. 2012, Yang et al. 2012,  
379 Stahlhut et al. 2015, Wang et al. 2015).

380

381 In agreement with previous studies, we demonstrate that upon encountering  
382 various types of cellular stress, TP53 in concert with additional factors bind  
383 and initiate transcription at the *miR34a* locus, thus increasing the levels of  
384 *miR34a* and, in addition, *miR34a* asRNA. We hypothesize that *miR34a*

385 asRNA may provide positive feedback for *miR34a* expression whereby  
386 *miR34a* asRNA serves as a scaffold for the recruitment of additional factors  
387 that facilitate polymerase II-mediated transcription, thus, increasing the  
388 expression of *miR34a* and driving the cell towards a reduction in growth factor  
389 signaling, senescence, and eventually apoptosis. On the other hand, in cells  
390 without functional *TP53*, other factors, which typically act independently or in  
391 concert with *TP53*, may initiate transcription of the *miR34a* locus. We believe  
392 that *miR34a* asRNA could potentially be interacting directly with one of these  
393 additional factors and recruiting it to the *miR34a* locus in order to drive  
394 *miR34a* transcription. This is especially plausible due to head-to-head  
395 orientation of the *miR34a* HG and asRNA, causing sequence complementarity  
396 between the RNA and the promoter DNA. Previous reports have also  
397 illustrated the ability of asRNAs to form hybrid DNA:RNA R-loops and, thus,  
398 facilitate an open chromatin structure and the transcription of the sense gene  
399 (Boque-Sastre et al. 2015). The fact that the p1 construct only contains a  
400 small portion of the *miR34a* asRNA transcript indicates that this portion is  
401 sufficient to give rise to at least a partial *miR34a* inducing response and  
402 therefore, indicates that *miR34a* asRNA may be able to facilitate *miR34a*  
403 expression independent of additional factors (**Fig 2d, Figure 2-Figure**  
404 **Supplement 2a**). Nevertheless, further work will need to be performed to  
405 ascertain the mechanism that is utilized in the case of *miR34a* asRNA.

406

407 An antisense transcript arising from the *miR34a* locus, *Lnc34a*, has been  
408 previously reported to negatively regulate the expression of *miR34a* (Wang et  
409 al. 2016). Although the *Lnc34a* and *miR34a* asRNA transcripts share some

410 sequence similarity, we believe them to be separate RNAs that are,  
411 potentially, different isoforms of the same gene. We thoroughly address our  
412 reasons for these beliefs and give appropriate supporting evidence in  
413 (**Supplementary Document 1**). The fact that *Lnc34a* and *miR34a* asRNA  
414 would appear to have opposing roles in their regulation of *miR34a* further  
415 underlines the complexity of the regulation at this locus.

416

417 Clinical trials utilizing *miR34a* replacement therapy have previously been  
418 conducted but, disappointingly, were terminated after adverse side effects of  
419 an immunological nature were observed in several of the patients (Slabakova  
420 et al. 2017). Although it is not presently clear if these side effects were caused  
421 by *miR34a* or the liposomal carrier used to deliver the miRNA, the multitude of  
422 evidence indicating *miR34a*'s crucial role in oncogenesis still makes its  
423 therapeutic induction an interesting strategy for therapy and needs further  
424 investigation. In summary, our results indicate that *miR34a* asRNA is a vital  
425 player in the regulation of *miR34a* and is especially important in typical  
426 examples of cellular stress encountered in cancer. We believe the  
427 conclusions drawn in this study to be essential in the progress towards  
428 developing a better understanding of the regulation of cancer-associated  
429 miRNAs and, specifically, the tumor suppressor *miR34a*.

430

## 431 **Materials and Methods**

### 432 **Cell Culture**

433 All cell lines were cultured at 5% CO<sub>2</sub> and 37° C with HEK293T, Saos2, and  
434 Skov3 cells cultured in DMEM high glucose (GE Healthcare Life Sciences,

435 Hyclone, UT, USA, Cat# SH30081), HCT116 and U2OS cells in McCoy's 5a  
436 (ThermoFisher Scientific, MA, USA, Cat# SH30200), and PC3 cells in RPMI  
437 (GE Healthcare Life Sciences, Hyclone, Cat# SH3009602) and 2 mM L-  
438 glutamine (GE Healthcare Life Sciences, Hyclone, Cat# SH3003402). All  
439 growth mediums were supplemented with 10% heat-inactivated FBS  
440 (ThermoFisher Scientific, Gibco, Cat# 12657029) and 50 µg/ml of  
441 streptomycin (ThermoFisher Scientific, Gibco, Cat# 15140122) and 50 µg/ml  
442 of penicillin (ThermoFisher Scientific, Gibco, Cat# 15140122).

443

444 **Bioinformatics, Data Availability, and Statistical Testing**

445 The USCS genome browser (Kent et al. 2002) was utilized for the  
446 bioinformatic evaluation of antisense transcription utilizing the RefSeq  
447 (O'Leary et al. 2016) gene annotation track.

448

449 All raw experimental data, code used for analysis, and supplementary  
450 methods are available for review at ([Serviss 2017](#)) and are provided as an R  
451 package. All analysis took place using the R statistical programming language  
452 (Team 2017) using multiple external packages that are all documented in the  
453 package associated with the article (Wilkins , Chang 2014, Wickham 2014,  
454 Wickham 2016, Allaire et al. 2017, Arnold 2017, Wickham 2017, Wickham  
455 2017, Wickham 2017, Xiao 2017, Xie 2017). The package facilitates  
456 replication of the operating system and package versions used for the original  
457 analysis, reproduction of each individual figure and figure supplement  
458 included in the article, and easy review of the code used for all steps of the  
459 analysis, from raw-data to figure.

460 The significance threshold (alpha) in this study was set to 0.05. Statistical

461 testing was performed using a Student's t-test unless otherwise specified.

462

463 **Coding Potential**

464 Protein-coding capacity was evaluated using the Coding-potential  
465 Assessment Tool (Wang et al. 2013) and Coding-potential Calculator (Kong et  
466 al. 2007) with default settings. Transcript sequences for use with Coding-  
467 potential Assessment Tool were downloaded from the UCSC genome  
468 browser using the Ensembl  
469 accessions: *HOTAIR* (ENST00000455246), *XIST* (ENST00000429829), β-  
470 actin (ENST00000331789), Tubulin (ENST00000427480),  
471 and *MYC* (ENST00000377970). Transcript sequences for use with Coding-  
472 potential Calculator were downloaded from the UCSC genome browser using  
473 the following IDs: *HOTAIR* (uc031qho.1), β-actin (uc003sq.4).

474

475 **shRNAs**

476 shRNA-expressing constructs were cloned into the U6M2 construct using the  
477 BgIII and KpnI restriction sites as previously described (Amarzguioui et al.  
478 2005). shRNA constructs were transfected using Lipofectamine 2000 or 3000  
479 (ThermoFisher Scientific, Cat# 12566014 and L3000015). The sequences  
480 targeting renilla is as follows: shRenilla 1.1 (AAT ACA CCG CGC TAC TGG  
481 C), shRenilla 2.1 (TAA CGG GAT TTC ACG AGG C).

482

483 **Lentiviral Particle production, infection, and selection**

484 Lentivirus production was performed as previously described in (Turner et al.  
485 2012). Briefly, HEK293T cells were transfected with viral and expression

486 constructs using Lipofectamine 2000 (ThermoFisher Scientific, Cat#  
487 12566014), after which viral supernatants were harvested 48 and 72 hours  
488 post-transfection. Viral particles were concentrated using PEG-IT solution  
489 (Systems Biosciences, CA, USA, Cat# LV825A-1) according to the  
490 manufacturer's recommendations. HEK293T cells were used for virus titration  
491 and GFP expression was evaluated 72hrs post-infection via flow cytometry  
492 (LSRII, BD Biosciences, CA, USA) after which TU/ml was calculated.

493

494 Stable lines were generated by infecting cells with a multiplicity of infection of  
495 1 after which 1-2 µM mycophenolic acid (Merck, NJ, USA, Cat# M5255)  
496 selection was initiated 48 hours post-infection. Cells were expanded as the  
497 selection process was monitored via flow cytometry analysis (LSRII, BD  
498 Biosciences) of GFP and selection was terminated once > 90% of the cells  
499 were GFP positive.

500

## 501 **Western Blotting**

502 Samples were lysed in 50 mM Tris-HCl (Sigma Aldrich, MO, USA, Cat#  
503 T2663), pH 7.4, 1% NP-40 (Sigma Aldrich, Cat# I8896), 150 mM NaCl (Sigma  
504 Aldrich, Cat# S5886), 1 mM EDTA (Promega, WI, USA, Cat# V4231), 1%  
505 glycerol (Sigma Aldrich, Cat# G5516), 100 µM vanadate (), protease inhibitor  
506 cocktail (Roche Diagnostics, Basel, Switzerland, Cat# 004693159001) and  
507 PhosSTOP (Roche Diagnostics, Cat# 04906837001). Lysates were subjected  
508 to SDS-PAGE and transferred to PVDF membranes. The proteins were  
509 detected by western blot analysis by using an enhanced chemiluminescence  
510 system (Western Lightning–ECL, PerkinElmer, Cat# NEL103001EA).

511 Antibodies used were specific for CCND1 1:1000 (Cell Signaling, Cat# 2926),  
512 and β-actin 1:5000 (Sigma-Aldrich, Cat# A5441). All western blot  
513 quantifications were performed using ImageJ (Schneider et al. 2012).

514

515 **Generation of U6-expressed miR34a AS Lentiviral Constructs**

516 The U6 promoter was amplified from the U6M2 cloning plasmid (Amarzguioui  
517 et al. 2005) and ligated into the Not1 restriction site of the pHIV7-IMPDH2  
518 vector (Turner et al. 2012). miR43a asRNA was PCR amplified and  
519 subsequently cloned into the Nhe1 and Pac1 restriction sites in the pHIV7-  
520 IMPDH2-U6 plasmid.

521

522 **Promoter Activity**

523 Cells were co-transfected with the renilla/firefly bidirectional promoter  
524 construct (Polson et al. 2011) and GFP by using Lipofectamine 2000 (Life  
525 Technologies, Cat# 12566014). The expression of GFP and luminescence  
526 was measured 24 h post transfection by using the Dual-Glo Luciferase Assay  
527 System (Promega, Cat# E2920) and detected by the GloMax-Multi+ Detection  
528 System (Promega, Cat# SA3030). The expression of luminescence was  
529 normalized to GFP.

530

531 **RNA Extraction and cDNA Synthesis**

532 For downstream SYBR green applications, RNA was extracted using the  
533 RNeasy mini kit (Qiagen, Venlo, Netherlands, Cat# 74106) and subsequently  
534 treated with DNase (Ambion Turbo DNA-free, ThermoFisher Scientific, Cat#  
535 AM1907). 500ng RNA was used for cDNA synthesis using MuMLV

536 (ThermoFisher Scientific, Cat# 28025013) and a 1:1 mix of oligo(dT) and  
537 random nanomers.

538

539 For analysis of miRNA expression with Taqman, samples were isolated with  
540 TRIzol reagent (ThermoFisher Scientific, Cat# 15596018) and further  
541 processed with the miRNeasy kit (Qiagen, Cat# 74106). cDNA synthesis was  
542 performed using the TaqMan MicroRNA Reverse Transcription Kit  
543 (ThermoFisher Scientific, Cat# 4366597) using the corresponding oligos  
544 according to the manufacturer's recommendations.

545

#### 546 **QPCR and PCR**

547 PCR was performed using the KAPA2G Fast HotStart ReadyMix PCR Kit  
548 (Kapa Biosystems, MA, USA, Cat# KK5601) with corresponding primers.  
549 QPCR was carried out using KAPA 2G SYBRGreen (Kapa Biosystems, Cat#  
550 KK4602) using the Applied Biosystems 7900HT machine with the cycling  
551 conditions: 95 °C for 3 min, 95 °C for 3 s, 60 °C for 30 s.

552

553 QPCR for miRNA expression analysis was performed according to the primer  
554 probe set manufacturers recommendations (ThermoFisher Scientific) and  
555 using the TaqMan Universal PCR Master Mix (ThermoFisher Scientific, Cat#  
556 4304437) with the same cycling scheme as above. Primer and probe sets for  
557 TaqMan were also purchased from ThermoFisher Scientific (Life  
558 Technologies at time of purchase, TaqMan® MicroRNA Assay, hsa-miR-34a,  
559 human, Cat# 4440887, Assay ID: 000426 and Control miRNA Assay, RNU48,  
560 human, Cat# 4440887, Assay ID: 001006).

561  
562 Primers for all PCR-based experiments are listed in **Supplementary**  
563 **Document 2** and arranged by figure.

564

565 **Bi-directional Promoter Cloning**

566 The overlapping region (p1) corresponds with the sequence previously  
567 published as the TP53 binding site in (Raver-Shapira et al. 2007) which we  
568 synthesized and cloned into the pLucRluc construct (Polson et al. 2011).

569

570 **Cell Cycle Distribution**

571 Cells were washed in PBS and fixed in 4% paraformaldehyde at room  
572 temperature overnight. Paraformaldehyde was removed, and cells were re-  
573 suspended in 95% EtOH. The samples were then rehydrated in distilled  
574 water, stained with DAPI and analyzed by flow cytometry on a LSRII (BD  
575 Biosciences) machine. Resulting cell cycle phases were quantified using the  
576 ModFit software (Verity Software House, ME, USA).

577

578 **3' Rapid Amplification of cDNA Ends**

579 3'-RACE was performed as described as previously in (Johnsson et al. 2013).  
580 Briefly, U2OS cell RNA was polyA-tailed using yeast polyA polymerase  
581 (ThermoFisher Scientific, Cat# 74225Z25KU) after which cDNA was  
582 synthesized using oligo(dT) primers. Nested-PCR was performed first using a  
583 forward primer in miR34a asRNA exon 1 and a tailed oligo(dT) primer  
584 followed by a second PCR using an alternate miR34a asRNA exon 1 primer  
585 and a reverse primer binding to the tail of the previously used oligo(dT)

586 primer. PCR products were gel purified and cloned the Strata Clone Kit  
587 (Agilent Technologies, CA, USA, Cat# 240205), and sequenced.

588

589 **Chromatin Immunoprecipitation**

590 The ChIP was performed as previously described in (Johnsson et al. 2013)  
591 with the following modifications. Cells were crosslinked in 1% formaldehyde  
592 (Merck, Cat# 1040039025), quenched with 0.125M glycine (Sigma Aldrich,  
593 Cat# G7126), and lysed in cell lysis buffer comprised of: 5mM PIPES (Sigma  
594 Aldrich, Cat# 80635), 85mM KCL (Merck, Cat# 4936), 0.5% NP40 (Sigma  
595 Aldrich, Cat# I8896), protease inhibitor (Roche Diagnostics, Cat#  
596 004693159001). Samples were then sonicated in 50mM TRIS-HCL pH 8.0  
597 (Sigma Aldrich, MO, USA, Cat# T2663) 10mM EDTA (Promega, WI, USA,  
598 Cat# V4231), 1% SDS (ThermoFisher Scientific, Cat# AM9822), and protease  
599 inhibitor (Roche Diagnostics, Cat# 004693159001) using a Bioruptor  
600 Sonicator (Diagenode, NJ, USA). Samples were incubated over night at 4°C  
601 with the *polII* antibody (Abcam, Cambridge, UK, Cat# ab5095) and  
602 subsequently pulled down with Salmon Sperm DNA/Protein A Agarose  
603 (Millipore, Cat# 16-157) beads. DNA was eluted in an elution buffer of 1%  
604 SDS (ThermoFisher Scientific, Cat# AM9822) 100mM NaHCO3 (Sigma  
605 Aldrich, Cat# 71631), followed by reverse crosslinking, RNaseA  
606 (ThermoFisher Scientific, Cat# 1692412) and protease K (New England  
607 Biolabs, MA, USA, Cat# P8107S) treatment. The DNA was eluted using  
608 Qiagen PCR purification kit (Cat# 28106).

609

610 **Confluency Analysis**

611 Cells were incubated in the Spark Multimode Microplate (Tecan) reader for 48  
612 hours at 37°C with 5% CO<sub>2</sub> in a humidity chamber. Confluency was  
613 measured every hour using bright-field microscopy and the percentage of  
614 confluency was reported via the plate reader's inbuilt algorithm. Percentage of  
615 confluency was normalized to the control sample in each condition (shown in  
616 figure) and then ranked. The rank was then used to construct a linear model of  
617 the dependency of the rank on the time and cell lines variables for each  
618 growth condition. Reported p-values are derived from the t-test, testing the  
619 null hypothesis that the coefficient estimate of the cell line variable is equal to  
620 0.

621

## 622 **Pharmacological Compounds**

623 Doxorubicin was purchased from Teva (cat. nr. 021361).

624

## 625 **Cellular Localization Analysis**

626 Quantified RNAseq data from 11 cell lines from the GRCh38 assembly was  
627 downloaded from the ENCODE project database and quantifications for  
628 miR34a asRNA (ENSG00000234546), GAPDH (ENSG00000111640), and  
629 MALAT1 (ENSG00000251562) were extracted. Cell lines for which data was  
630 downloaded include: A549, GM12878, HeLa-S3, HepG2, HT1080, K562  
631 MCF-7, NCI-H460, SK-MEL-5, SK-N-DZ, SK-N-SH. Initial exploratory analysis  
632 revealed that several cell lines should be removed from the analysis due to a)  
633 a larger proportion of GAPDH in the nucleus than cytoplasm or b) variation of  
634 miR34a asRNA expression is too large to draw conclusions, or c) they have  
635 no or low (<6 TPM) miR34a asRNA expression. Furthermore, only

636 polyadenylated libraries were used in the final analysis, due to the fact that  
637 the cellular compartment enrichment was improved in these samples. All  
638 analyzed genes are reported to be polyadenylated. In addition, only samples  
639 with 2 biological replicates were retained. For each cell type, gene, and  
640 biological replicate the fraction of transcripts per million (TPM) in each cellular  
641 compartment was calculated as the fraction of TPM in the specific  
642 compartment by the total TPM. The mean and standard deviation for the  
643 fraction was subsequently calculated for each cell type and cellular  
644 compartment and this information was represented in the final figure.

645

#### 646 **CAGE Analysis**

647 All available CAGE data from the ENCODE project (Consortium 2012) for 36  
648 cell lines was downloaded from the UCSC genome browser (Kent et al. 2002)  
649 for genome version hg19. Of these, 28 cell lines had CAGE transcription start  
650 sites (TSS) mapping to the plus strand of chromosome 1 and in regions  
651 corresponding to 200 base pairs upstream of the *lnc34a* start site (9241796 -  
652 200) and 200 base pairs upstream of the GENCODE  
653 annotated *miR34a* asRNA start site (9242263 + 200). These cell lines  
654 included: HFDPC, H1-hESC, HMEpC, HAoEC, HPIEpC, HSaVEC, GM12878,  
655 hMSC-BM, HUVEC, AG04450, hMSC-UC, IMR90, NHDF, SK-N-SH\_RA, BJ,  
656 HOB, HPC-PL, HAoAF, NHEK, HVMF, HWP, MCF-7, HepG2, hMSC-AT,  
657 NHEM.f\_M2, SkMC, NHEM\_M2, and HCH. In total 74 samples were included.  
658 17 samples were polyA-, 47 samples were polyA+, and 10 samples were total  
659 RNA. In addition, 34 samples were whole cell, 15 enriched for the cytosolic  
660 fraction, 15 enriched for the nucleolus, and 15 enriched for the nucleus. All

661 CAGE transcription start sites were plotted and the RPKM of the individual  
662 reads was used to color each read to indicate their relative abundance. In  
663 cases where CAGE TSS spanned identical regions, the RPMKs of the regions  
664 were summed and represented as one CAGE TSS in the figure. In addition, a  
665 density plot shows the distribution of the CAGE reads in the specified  
666 interval.

667

#### 668 **Splice Junction Analysis**

669 All available whole cell (i.e. non-fractionated) spliced read data originating  
670 from the Cold Spring Harbor Lab in the ENCODE project (Consortium 2012)  
671 for 38 cell lines was downloaded from the UCSC genome browser (Kent et al.  
672 2002). Of these cell lines, 36 had spliced reads mapping to the plus strand of  
673 chromosome 1 and in the region between the *lnc34a* start (9241796) and  
674 transcription termination (9257102) site (note that *miR34a* asRNA resides  
675 totally within this region). Splice junctions from the following cell lines were  
676 included in the final figure: A549, Ag04450, Bj, CD20, CD34 mobilized,  
677 Gm12878, H1hesc, Haoaf, Haoec, Hch, Helas3, Hepg2, Hfdpc, Hmec,  
678 Hmepc, Hmescat, Hmscbm, Hmscuc, Hob, Hpcpl, Hpiepc, Hsavec, Hsmm,  
679 Huvec, Hvmf, Hwp, Imr90, Mcf7, Monocd14, Nhdf, Nhek, Nhemfm2,  
680 Nhemm2, Nhlf, Skmc, and Sknsh. All splice junctions were included in the  
681 figure and colored according to the number of reads corresponding to each. In  
682 cases where identical reads were detected multiple times, the read count was  
683 summed and represented as one read in the figure.

684

#### 685 **TCGA Expression and Correlation Analysis**

686 Erik/Jimmy should probably take this.

687

## 688 **Acknowledgments**

689

## 690 **Competing Interests**

691

692 The authors declare no competing interests.

693

## 694 **Funding**

695

696 This work has been supported by the Swedish Research Council [521-2012-2037],  
697 Swedish Cancer Society [150768], Cancer Research Foundations of Radiumhemmet  
698 [144063] and the Swedish Childhood Cancer Foundation [PR2015-0009].

699

700

## 701 **Figure Supplements**

702

703 Figure 1-Supplement 1: TCAG expression levels and correlation analysis  
704 statistics.

705

706 Figure 1-Supplement 2: Molecular characteristics of miR34a asRNA.

707

708 Figure 2-Supplement 1: A schematic representation of the p1 construct.

709

710 Figure 2-Supplement 2: Evaluating the effects of miR34a asRNA down-  
711 regulation.

712

713 Figure 3-Supplement 1: Physiological relevance of miR34a asRNA  
714 overexpression.

715

716 Figure 3-Supplement 2: Effects of miR34a asRNA overexpression on cyclin  
717 D1.

718

719 Supplementary Document 1: Evaluating the relationship between miR34a  
720 asRNA and lnc34a.

721

722 Supplementary Document 2: A table of primers used in this study.

723

## 724 **Data Supplements**

725

726 Figure 1C-Source Data 1

727 Figure 2B-Source Data 1

728 Figure 2C-Source Data 1

729    Figure 2D-Source Data 1

730    Figure 3A- Source Data 1

731

732    Figure 3B-Source Data 1

733

734    Figure 3C-Source Data 1

735

736    Figure 3D-Source Data 1

737

738

739

740

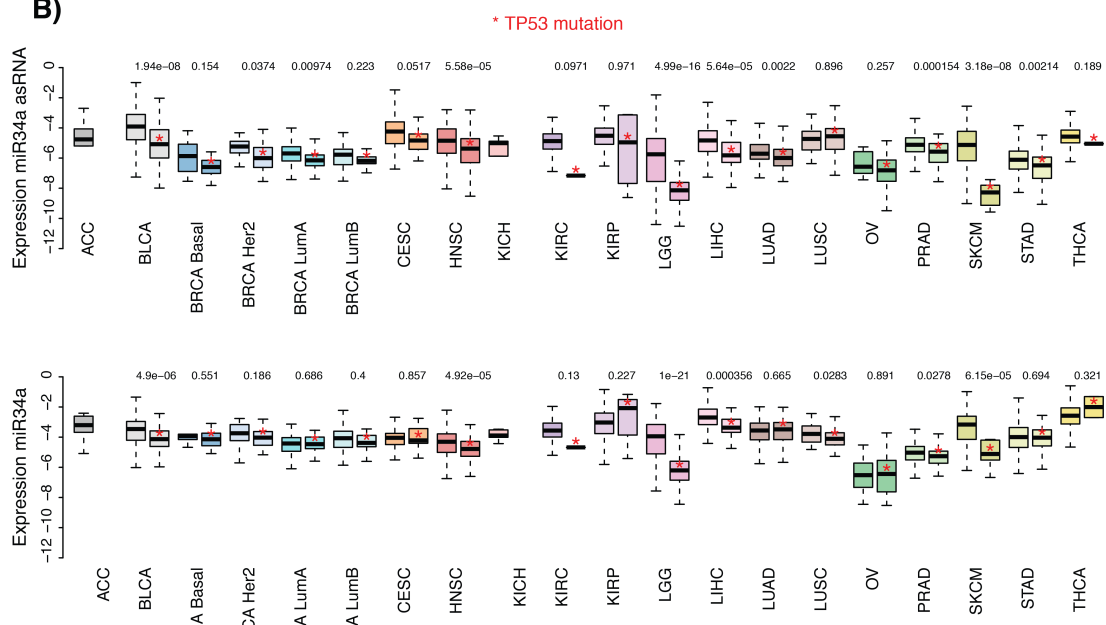
741 **Supplementary Figures**

742

**A)**

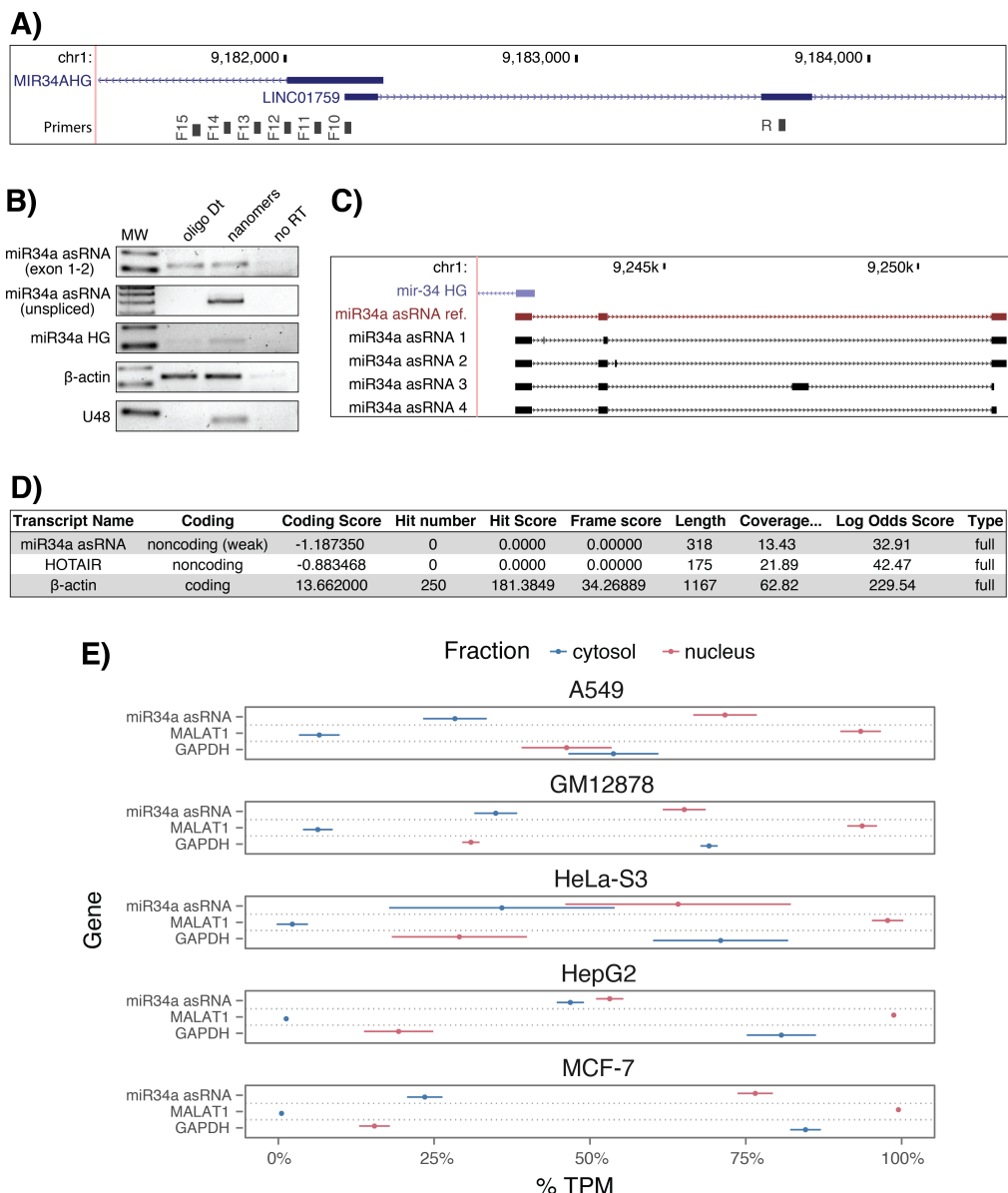
cancer	all n	all rho	all p	TP53wt n	TP53wt rho	TP53wt p	TP53mut n	TP53mut rho	TP53mut p
ACC	10	5.52e-01	1.04e-01	10	5.52e-01	1.04e-01	NA	NA	NA
BLCA	228	5.15e-01	7.89e-17	134	4.53e-01	3.86e-08	94	4.27e-01	1.73e-05
BRCA Basal	42	5.74e-01	9.54e-05	10	6.24e-01	6.02e-02	32	5.74e-01	7.41e-04
BRCA Her2	44	1.47e-01	3.39e-01	12	2.24e-01	4.85e-01	32	6.82e-02	7.10e-01
BRCA LumA	199	3.41e-01	8.22e-07	177	3.43e-01	2.96e-06	22	4.86e-01	2.31e-02
BRCA LumB	70	1.71e-01	1.57e-01	61	1.48e-01	2.53e-01	9	1.67e-01	6.78e-01
CESC	156	1.39e-01	8.37e-02	145	1.60e-01	5.45e-02	11	-4.55e-02	9.03e-01
HNSC	313	5.37e-01	8.38e-25	123	6.08e-01	0.00e+00	190	4.47e-01	9.68e-11
KICH	5	6.00e-01	3.50e-01	5	6.00e-01	3.50e-01	NA	NA	NA
KIRC	142	3.49e-01	2.06e-05	141	3.37e-01	4.41e-05	NA	NA	NA
KIRP	167	4.51e-01	9.16e-10	163	4.48e-01	2.04e-09	4	8.00e-01	3.33e-01
LGG	271	6.33e-01	9.92e-32	76	7.28e-01	0.00e+00	195	3.87e-01	2.26e-08
LIHC	153	5.63e-01	3.64e-14	114	5.16e-01	4.18e-09	39	4.55e-01	3.95e-03
LUAD	234	2.82e-01	1.15e-05	128	3.61e-01	2.87e-05	106	2.27e-01	1.91e-02
LUSC	139	2.29e-01	6.74e-03	42	4.17e-02	7.93e-01	97	3.29e-01	9.91e-04
OV	56	2.33e-01	8.37e-02	10	8.42e-01	4.46e-03	46	1.46e-01	3.31e-01
PRAD	413	4.66e-01	1.33e-23	375	4.59e-01	6.13e-21	38	4.50e-01	4.58e-03
SKCM	165	6.48e-01	5.43e-21	152	6.10e-01	7.85e-17	13	4.34e-01	1.40e-01
STAD	225	3.72e-01	8.23e-09	145	3.67e-01	5.71e-06	80	4.20e-01	1.03e-04
THCA	469	4.58e-01	1.07e-25	467	4.62e-01	4.06e-26	NA	NA	NA

**B)**



743  
744

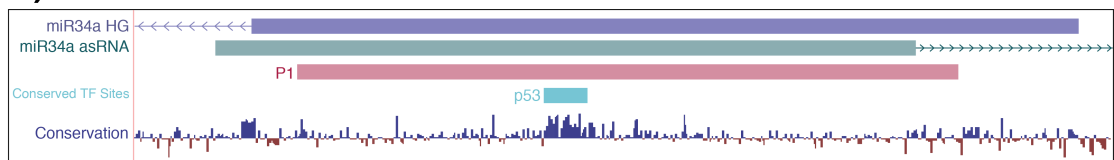
**Figure 1 Supplement 1: TCAG expression levels and correlation analysis statistics.** A) Spearman's rho and p-values (p) from the correlation analysis investigating the correlation between miR34a and miR34a asRNA expression in TP53 wild type (wt) and mutated (mut) samples within TCGA cancer types. B) Expression levels of miR34a and miR34a asRNA in TP53 wt and nonsynonymous mutation samples. Bladder Urothelial Carcinoma (BLCA), Breast invasive carcinoma (BRCA), Head and Neck squamous cell carcinoma (HNSC), Lower Grade Glioma (LGG), Liver hepatocellular carcinoma (LIHC), Lung adenocarcinoma (LUAD), Lung squamous cell carcinoma (LUSC), Ovarian serous cystadenocarcinoma (OV), Prostate adenocarcinoma (PRAD), Skin Cutaneous Melanoma (SKCM), Stomach adenocarcinoma (STAD).



754  
755  
756  
757  
758  
759  
760  
761  
762  
763  
764  
765  
766

**Figure 1 Supplement 2: Molecular characteristics of miR34a asRNA.** **A)** A schematic representation of the primer placement in the primer walk assay. **B)** Polyadenylation status of spliced and unspliced miR34a asRNA in HEK293T cells. **C)** Sequencing results from the analysis of *miR34a* asRNA isoforms in U2OS cells. *miR34a* AS ref. refers to the full length transcript as defined by the 3'-RACE and primer walk assay. **D)** Analysis of coding potential of the *miR34a* asRNA transcript using the Coding-potential Calculator. **E)** RNAseq data from five fractionated cell lines in the ENCODE project showing the percentage of transcripts per million (TPM) for miR34a asRNA. MALAT1 (nuclear localization) and GAPDH (cytoplasmic localization) are included as fractionation controls. Points represent the mean and horizontal lines represent the standard deviation from two biological replicates.

**A)**

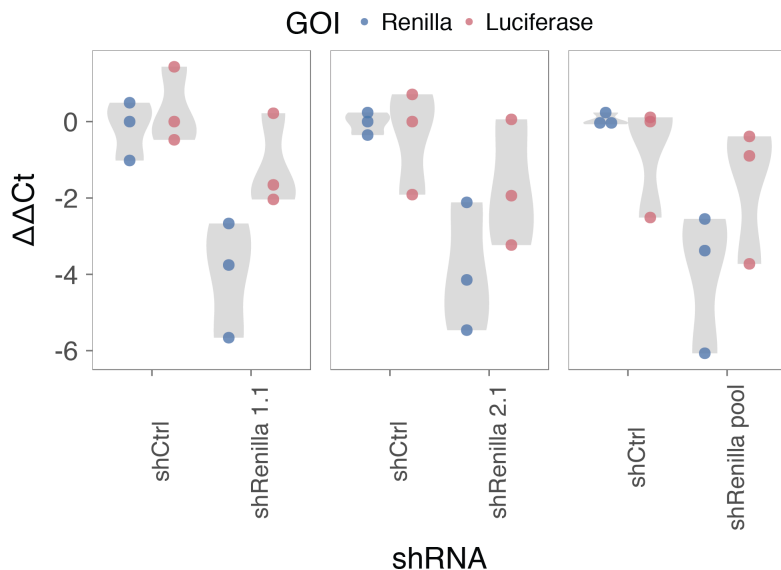


**B)**



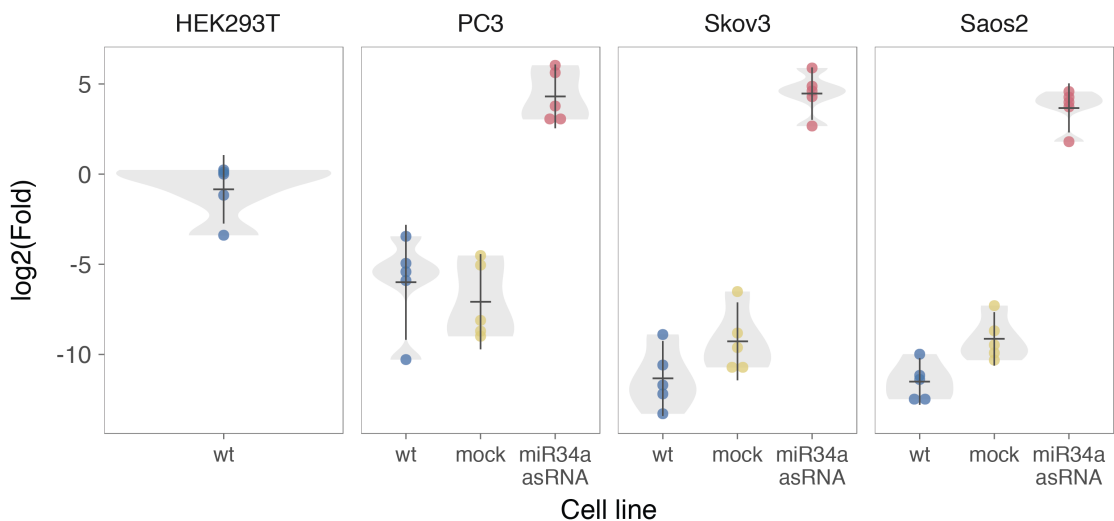
767  
768  
769  
770  
771  
772

**Figure 2 Supplement 1: A schematic representation of the p1 construct. A)** A UCSC genome browser illustration indicating the location of the promoter region cloned into the p1 construct including the conserved *TP53*-binding site. **B)** A representative picture of the p1 construct including forward (F) and reverse (R) primer locations and the renilla shRNA targeting site.



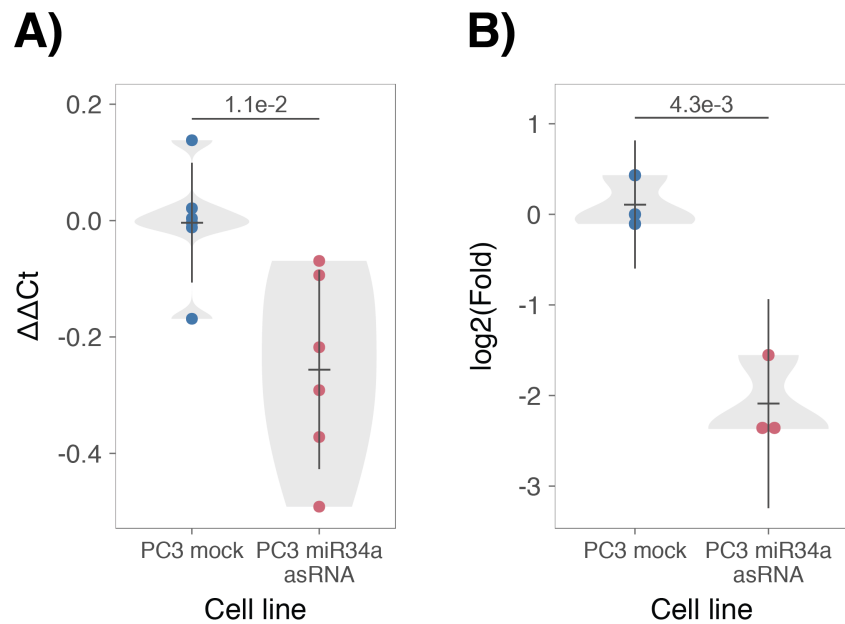
773  
774  
775  
776  
777  
778

**Figure 2 Supplement 2: Evaluating the effects of miR34a asRNA down-regulation.** HEK293T cells were co-transfected with the P1 construct and either shRenilla or shControl. Renilla and luciferase levels were measured with Q-PCR 48 hours after transfection. Individual points represent independent experiments with the gray shadow indicating the density of the points.



779  
780

781 **Figure 3 Supplement 1: Physiological relevance of miR34a asRNA overexpression.** Comparison  
782 of *miR34a* asRNA expression in HEK293T cells (high endogenous *miR34a* asRNA), and the wild-type  
783 (wt), mock, and *miR34a* asRNA over-expressing stable cell lines.



784  
785  
786  
787  
788

**Figure 3 Supplement 2: Effects of miR34a asRNA overexpression on cyclin D1.** CCND1 expression (A) and western blot quantification of protein levels (B) in *miR34a* asRNA over-expressing PC3 stable cell lines.

789 **References**

- 790
- 791 Agostini, M., P. Tucci, R. Killick, E. Candi, B. S. Sayan, P. Rivetti di Val Cervo, P.  
792 Nicotera, F. McKeon, R. A. Knight, T. W. Mak and G. Melino (2011). "Neuronal  
793 differentiation by TAp73 is mediated by microRNA-34a regulation of synaptic  
794 protein targets." *Proc Natl Acad Sci U S A* **108**(52): 21093-21098. DOI:  
795 10.1073/pnas.1112061109
- 796
- 797 Ahn, Y. H., D. L. Gibbons, D. Chakravarti, C. J. Creighton, Z. H. Rizvi, H. P. Adams, A.  
798 Pertsemlidis, P. A. Gregory, J. A. Wright, G. J. Goodall, E. R. Flores and J. M. Kurie  
799 (2012). "ZEB1 drives prometastatic actin cytoskeletal remodeling by  
800 downregulating miR-34a expression." *J Clin Invest* **122**(9): 3170-3183. DOI:  
801 10.1172/JCI63608
- 802
- 803 Allaire, J., Y. Xie, J. McPherson, J. Luraschi, K. Ushey, A. Atkins, H. Wickham, J.  
804 Cheng and W. Chang (2017). rmarkdown: Dynamic Documents for R. R package  
805 version 1.8. <https://CRAN.R-project.org/package=rmarkdown>
- 806
- 807 Amarzguioui, M., J. J. Rossi and D. Kim (2005). "Approaches for chemically  
808 synthesized siRNA and vector-mediated RNAi." *FEBS Lett* **579**(26): 5974-5981.  
809 DOI: 10.1016/j.febslet.2005.08.070
- 810
- 811 Arnold, J. B. (2017). ggthemes: Extra Themes, Scales and Geoms for 'ggplot2'. R  
812 package version 3.4.0. <https://CRAN.R-project.org/package=ggthemes>
- 813
- 814 Ashouri, A., V. I. Sayin, J. Van den Eynden, S. X. Singh, T. Papagiannakopoulos and  
815 E. Larsson (2016). "Pan-cancer transcriptomic analysis associates long non-  
816 coding RNAs with key mutational driver events." *Nature Communications* **7**:  
817 13197. DOI: 10.1038/ncomms13197
- 818
- 819 Balbin, O. A., R. Malik, S. M. Dhanasekaran, J. R. Prensner, X. Cao, Y. M. Wu, D.  
820 Robinson, R. Wang, G. Chen, D. G. Beer, A. I. Nesvizhskii and A. M. Chinnaian  
821 (2015). "The landscape of antisense gene expression in human cancers." *Genome  
822 Res* **25**(7): 1068-1079. DOI: 10.1101/gr.180596.114
- 823
- 824 Boque-Sastre, R., M. Soler, C. Oliveira-Mateos, A. Portela, C. Moutinho, S. Sayols, A.  
825 Villanueva, M. Esteller and S. Guil (2015). "Head-to-head antisense transcription  
826 and R-loop formation promotes transcriptional activation." *Proc Natl Acad Sci U  
827 SA* **112**(18): 5785-5790. DOI: 10.1073/pnas.1421197112
- 828
- 829 Chang, T. C., D. Yu, Y. S. Lee, E. A. Wentzel, D. E. Arking, K. M. West, C. V. Dang, A.  
830 Thomas-Tikhonenko and J. T. Mendell (2008). "Widespread microRNA  
831 repression by Myc contributes to tumorigenesis." *Nat Genet* **40**(1): 43-50. DOI:  
832 10.1038/ng.2007.30
- 833
- 834 Chang, W. (2014). extrafont: Tools for using fonts. R package version 0.17.  
835 <https://CRAN.R-project.org/package=extrafont>
- 836

- 837 Chen, J., M. Sun, W. J. Kent, X. Huang, H. Xie, W. Wang, G. Zhou, R. Z. Shi and J. D.  
838 Rowley (2004). "Over 20% of human transcripts might form sense-antisense  
839 pairs." *Nucleic Acids Res* **32**(16): 4812-4820. DOI: 10.1093/nar/gkh818
- 840
- 841 Cheng, J., L. Zhou, Q. F. Xie, H. Y. Xie, X. Y. Wei, F. Gao, C. Y. Xing, X. Xu, L. J. Li and S.  
842 S. Zheng (2010). "The impact of miR-34a on protein output in hepatocellular  
843 carcinoma HepG2 cells." *Proteomics* **10**(8): 1557-1572. DOI:  
844 10.1002/pmic.200900646
- 845
- 846 Chim, C. S., K. Y. Wong, Y. Qi, F. Loong, W. L. Lam, L. G. Wong, D. Y. Jin, J. F. Costello  
847 and R. Liang (2010). "Epigenetic inactivation of the miR-34a in hematological  
848 malignancies." *Carcinogenesis* **31**(4): 745-750. DOI: 10.1093/carcin/bgq033
- 849
- 850 Cole, K. A., E. F. Attiyeh, Y. P. Mosse, M. J. Laquaglia, S. J. Diskin, G. M. Brodeur and  
851 J. M. Maris (2008). "A functional screen identifies miR-34a as a candidate  
852 neuroblastoma tumor suppressor gene." *Mol Cancer Res* **6**(5): 735-742. DOI:  
853 10.1158/1541-7786.MCR-07-2102
- 854
- 855 Conley, A. B. and I. K. Jordan (2012). "Epigenetic regulation of human cis-natural  
856 antisense transcripts." *Nucleic Acids Res* **40**(4): 1438-1445. DOI:  
857 10.1093/nar/gkr1010
- 858
- 859 Consortium, E. P. (2012). "An integrated encyclopedia of DNA elements in the  
860 human genome." *Nature* **489**(7414): 57-74. DOI: 10.1038/nature11247
- 861
- 862 Ding, N., H. Wu, T. Tao and E. Peng (2017). "NEAT1 regulates cell proliferation  
863 and apoptosis of ovarian cancer by miR-34a-5p/BCL2." *Onco Targets Ther* **10**:  
864 4905-4915. DOI: 10.2147/OTT.S142446
- 865
- 866 Djebali, S., C. A. Davis, A. Merkel, A. Dobin, T. Lassmann, A. Mortazavi, A. Tanzer, J.  
867 Lagarde, W. Lin, F. Schlesinger, C. Xue, G. K. Marinov, J. Khatun, B. A. Williams, C.  
868 Zaleski, J. Rozowsky, M. Roder, F. Kokocinski, R. F. Abdelhamid, T. Alioto, I.  
869 Antoshechkin, M. T. Baer, N. S. Bar, P. Batut, K. Bell, I. Bell, S. Chakrabortty, X.  
870 Chen, J. Chrast, J. Curado, T. Derrien, J. Drenkow, E. Dumais, J. Dumais, R.  
871 Duttagupta, E. Falconnet, M. Fastuca, K. Fejes-Toth, P. Ferreira, S. Foissac, M. J.  
872 Fullwood, H. Gao, D. Gonzalez, A. Gordon, H. Gunawardena, C. Howald, S. Jha, R.  
873 Johnson, P. Kapranov, B. King, C. Kingswood, O. J. Luo, E. Park, K. Persaud, J. B.  
874 Preall, P. Ribeca, B. Risk, D. Robyr, M. Sammeth, L. Schaffer, L. H. See, A. Shahab, J.  
875 Skancke, A. M. Suzuki, H. Takahashi, H. Tilgner, D. Trout, N. Walters, H. Wang, J.  
876 Wrobel, Y. Yu, X. Ruan, Y. Hayashizaki, J. Harrow, M. Gerstein, T. Hubbard, A.  
877 Reymond, S. E. Antonarakis, G. Hannon, M. C. Giddings, Y. Ruan, B. Wold, P.  
878 Carninci, R. Guigo and T. R. Gingeras (2012). "Landscape of transcription in  
879 human cells." *Nature* **489**(7414): 101-108. DOI: 10.1038/nature11233
- 880
- 881 Gallardo, E., A. Navarro, N. Vinolas, R. M. Marrades, T. Diaz, B. Gel, A. Quera, E.  
882 Bandres, J. Garcia-Foncillas, J. Ramirez and M. Monzo (2009). "miR-34a as a  
883 prognostic marker of relapse in surgically resected non-small-cell lung cancer."  
884 *Carcinogenesis* **30**(11): 1903-1909. DOI: 10.1093/carcin/bgp219
- 885

- 886 Hunten, S., M. Kaller, F. Drepper, S. Oeljeklaus, T. Bonfert, F. Erhard, A. Dueck, N.  
887 Eichner, C. C. Friedel, G. Meister, R. Zimmer, B. Warscheid and H. Hermeking  
888 (2015). "p53-Regulated Networks of Protein, mRNA, miRNA, and lncRNA  
889 Expression Revealed by Integrated Pulsed Stable Isotope Labeling With Amino  
890 Acids in Cell Culture (pSILAC) and Next Generation Sequencing (NGS) Analyses."  
891 Mol Cell Proteomics **14**(10): 2609-2629. DOI: 10.1074/mcp.M115.050237
- 892
- 893 International Human Genome Sequencing, C. (2004). "Finishing the euchromatic  
894 sequence of the human genome." Nature **431**(7011): 931-945. DOI:  
895 10.1038/nature03001
- 896
- 897 Johnsson, P., A. Ackley, L. Vidarsdottir, W. O. Lui, M. Corcoran, D. Grander and K.  
898 V. Morris (2013). "A pseudogene long-noncoding-RNA network regulates PTEN  
899 transcription and translation in human cells." Nat Struct Mol Biol **20**(4): 440-  
900 446. DOI: 10.1038/nsmb.2516
- 901
- 902 Katayama, S., Y. Tomaru, T. Kasukawa, K. Waki, M. Nakanishi, M. Nakamura, H.  
903 Nishida, C. C. Yap, M. Suzuki, J. Kawai, H. Suzuki, P. Carninci, Y. Hayashizaki, C.  
904 Wells, M. Frith, T. Ravasi, K. C. Pang, J. Hallinan, J. Mattick, D. A. Hume, L. Lipovich,  
905 S. Batalov, P. G. Engstrom, Y. Mizuno, M. A. Faghihi, A. Sandelin, A. M. Chalk, S.  
906 Mottagui-Tabar, Z. Liang, B. Lenhard, C. Wahlestedt, R. G. E. R. Group, G. Genome  
907 Science and F. Consortium (2005). "Antisense transcription in the mammalian  
908 transcriptome." Science **309**(5740): 1564-1566. DOI: 10.1126/science.1112009
- 909
- 910 Kent, W. J., C. W. Sugnet, T. S. Furey, K. M. Roskin, T. H. Pringle, A. M. Zahler and D.  
911 Haussler (2002). "The human genome browser at UCSC." Genome Res **12**(6):  
912 996-1006. DOI: 10.1101/gr.229102. Article published online before print in May  
913 2002
- 914
- 915 Kim, K. H., H. J. Kim and T. R. Lee (2017). "Epidermal long non-coding RNAs are  
916 regulated by ultraviolet irradiation." Gene **637**: 196-202. DOI:  
917 10.1016/j.gene.2017.09.043
- 918
- 919 Kong, L., Y. Zhang, Z. Q. Ye, X. Q. Liu, S. Q. Zhao, L. Wei and G. Gao (2007). "CPC:  
920 assess the protein-coding potential of transcripts using sequence features and  
921 support vector machine." Nucleic Acids Res **35**(Web Server issue): W345-349.  
922 DOI: 10.1093/nar/gkm391
- 923
- 924 Lal, A., M. P. Thomas, G. Altschuler, F. Navarro, E. O'Day, X. L. Li, C. Concepcion, Y.  
925 C. Han, J. Thiery, D. K. Rajani, A. Deutsch, O. Hofmann, A. Ventura, W. Hide and J.  
926 Lieberman (2011). "Capture of microRNA-bound mRNAs identifies the tumor  
927 suppressor miR-34a as a regulator of growth factor signaling." PLoS Genet **7**(11):  
928 e1002363. DOI: 10.1371/journal.pgen.1002363
- 929
- 930 Leveille, N., C. A. Melo, K. Rooijers, A. Diaz-Lagares, S. A. Melo, G. Korkmaz, R.  
931 Lopes, F. Akbari Moqadam, A. R. Maia, P. J. Wijchers, G. Geeven, M. L. den Boer, R.  
932 Kalluri, W. de Laat, M. Esteller and R. Agami (2015). "Genome-wide profiling of  
933 p53-regulated enhancer RNAs uncovers a subset of enhancers controlled by a  
934 lncRNA." Nature Communications **6**: 6520. DOI: 10.1038/ncomms7520

- 935  
936 Liu, C., K. Kelnar, B. Liu, X. Chen, T. Calhoun-Davis, H. Li, L. Patrawala, H. Yan, C.  
937 Jeter, S. Honorio, J. F. Wiggins, A. G. Bader, R. Fagin, D. Brown and D. G. Tang  
938 (2011). "The microRNA miR-34a inhibits prostate cancer stem cells and  
939 metastasis by directly repressing CD44." *Nat Med* **17**(2): 211-215. DOI:  
940 10.1038/nm.2284  
941  
942 Memczak, S., M. Jens, A. Elefsinioti, F. Torti, J. Krueger, A. Rybak, L. Maier, S. D.  
943 Mackowiak, L. H. Gregersen, M. Munschauer, A. Loewer, U. Ziebold, M.  
944 Landthaler, C. Kocks, F. le Noble and N. Rajewsky (2013). "Circular RNAs are a  
945 large class of animal RNAs with regulatory potency." *Nature* **495**(7441): 333-  
946 338. DOI: 10.1038/nature11928  
947  
948 O'Leary, N. A., M. W. Wright, J. R. Brister, S. Ciufo, D. Haddad, R. McVeigh, B.  
949 Rajput, B. Robbertse, B. Smith-White, D. Ako-Adjei, A. Astashyn, A. Badretdin, Y.  
950 Bao, O. Blinkova, V. Brover, V. Chetvernin, J. Choi, E. Cox, O. Ermolaeva, C. M.  
951 Farrell, T. Goldfarb, T. Gupta, D. Haft, E. Hatcher, W. Hlavina, V. S. Joardar, V. K.  
952 Kodali, W. Li, D. Maglott, P. Masterson, K. M. McGarvey, M. R. Murphy, K. O'Neill,  
953 S. Pujar, S. H. Rangwala, D. Rausch, L. D. Riddick, C. Schoch, A. Shkeda, S. S. Storz,  
954 H. Sun, F. Thibaud-Nissen, I. Tolstoy, R. E. Tully, A. R. Vatsan, C. Wallin, D. Webb,  
955 W. Wu, M. J. Landrum, A. Kimchi, T. Tatusova, M. DiCuccio, P. Kitts, T. D. Murphy  
956 and K. D. Pruitt (2016). "Reference sequence (RefSeq) database at NCBI: current  
957 status, taxonomic expansion, and functional annotation." *Nucleic Acids Res*  
958 **44**(D1): D733-745. DOI: 10.1093/nar/gkv1189  
959  
960 Ozsolak, F., P. Kapranov, S. Foissac, S. W. Kim, E. Fishilevich, A. P. Monaghan, B.  
961 John and P. M. Milos (2010). "Comprehensive polyadenylation site maps in yeast  
962 and human reveal pervasive alternative polyadenylation." *Cell* **143**(6): 1018-  
963 1029. DOI: 10.1016/j.cell.2010.11.020  
964  
965 Polson, A., E. Durrett and D. Reisman (2011). "A bidirectional promoter reporter  
966 vector for the analysis of the p53/WDR79 dual regulatory element." *Plasmid*  
967 **66**(3): 169-179. DOI: 10.1016/j.plasmid.2011.08.004  
968  
969 Rashi-Elkeles, S., H. J. Warnatz, R. Elkon, A. Kupershtein, Y. Chobod, A. Paz, V.  
970 Amstislavskiy, M. Sultan, H. Safer, W. Nietfeld, H. Lehrach, R. Shamir, M. L. Yaspo  
971 and Y. Shiloh (2014). "Parallel profiling of the transcriptome, cistrome, and  
972 epigenome in the cellular response to ionizing radiation." *Sci Signal* **7**(325): rs3.  
973 DOI: 10.1126/scisignal.2005032  
974  
975 Raver-Shapira, N., E. Marciano, E. Meiri, Y. Spector, N. Rosenfeld, N. Moskovits, Z.  
976 Bentwich and M. Oren (2007). "Transcriptional activation of miR-34a  
977 contributes to p53-mediated apoptosis." *Mol Cell* **26**(5): 731-743. DOI:  
978 10.1016/j.molcel.2007.05.017  
979  
980 Rinn, J. L., M. Kertesz, J. K. Wang, S. L. Squazzo, X. Xu, S. A. Brugmann, L. H.  
981 Goodnough, J. A. Helms, P. J. Farnham, E. Segal and H. Y. Chang (2007).  
982 "Functional demarcation of active and silent chromatin domains in human HOX

983 loci by noncoding RNAs." *Cell* **129**(7): 1311-1323. DOI:  
984 10.1016/j.cell.2007.05.022  
985  
986 Rokavec, M., M. G. Oner, H. Li, R. Jackstadt, L. Jiang, D. Lodygin, M. Kaller, D. Horst,  
987 P. K. Ziegler, S. Schwitalla, J. Slotta-Huspenina, F. G. Bader, F. R. Greten and H.  
988 Hermeking (2015). "Corrigendum. IL-6R/STAT3/miR-34a feedback loop  
989 promotes EMT-mediated colorectal cancer invasion and metastasis." *J Clin Invest*  
990 **125**(3): 1362. DOI: 10.1172/JCI81340  
991  
992 Schneider, C. A., W. S. Rasband and K. W. Eliceiri (2012). "NIH Image to ImageJ:  
993 25 years of image analysis." *Nat Methods* **9**(7): 671-675.  
994  
995 Serviss, J. T. (2017). miR34AasRNaproject.  
996 [https://github.com/GranderLab/miR34a\\_asRNA\\_project](https://github.com/GranderLab/miR34a_asRNA_project)  
997  
998 Serviss, J. T., P. Johnsson and D. Grander (2014). "An emerging role for long non-  
999 coding RNAs in cancer metastasis." *Front Genet* **5**: 234. DOI:  
1000 10.3389/fgene.2014.00234  
1001  
1002 Slabakova, E., Z. Culig, J. Remsik and K. Soucek (2017). "Alternative mechanisms  
1003 of miR-34a regulation in cancer." *Cell Death Dis* **8**(10): e3100. DOI:  
1004 10.1038/cddis.2017.495  
1005  
1006 Stahlhut, C. and F. J. Slack (2015). "Combinatorial Action of MicroRNAs let-7 and  
1007 miR-34 Effectively Synergizes with Erlotinib to Suppress Non-small Cell Lung  
1008 Cancer Cell Proliferation." *Cell Cycle* **14**(13): 2171-2180. DOI:  
1009 10.1080/15384101.2014.1003008  
1010  
1011 Su, X., D. Chakravarti, M. S. Cho, L. Liu, Y. J. Gi, Y. L. Lin, M. L. Leung, A. El-Naggar,  
1012 C. J. Creighton, M. B. Suraokar, I. Wistuba and E. R. Flores (2010). "TAp63  
1013 suppresses metastasis through coordinate regulation of Dicer and miRNAs."  
1014 *Nature* **467**(7318): 986-990. DOI: 10.1038/nature09459  
1015  
1016 Sun, F., H. Fu, Q. Liu, Y. Tie, J. Zhu, R. Xing, Z. Sun and X. Zheng (2008).  
1017 "Downregulation of CCND1 and CDK6 by miR-34a induces cell cycle arrest."  
1018 *FEBS Lett* **582**(10): 1564-1568. DOI: 10.1016/j.febslet.2008.03.057  
1019  
1020 Tarasov, V., P. Jung, B. Verdoodt, D. Lodygin, A. Epanchintsev, A. Menssen, G.  
1021 Meister and H. Hermeking (2007). "Differential regulation of microRNAs by p53  
1022 revealed by massively parallel sequencing: miR-34a is a p53 target that induces  
1023 apoptosis and G1-arrest." *Cell Cycle* **6**(13): 1586-1593. DOI:  
1024 10.4161/cc.6.13.4436  
1025  
1026 Team, R. C. (2017). "R: A Language and Environment for Statistical Computing."  
1027 from <https://www.R-project.org/>.  
1028  
1029 Turner, A. M., A. M. Ackley, M. A. Matrone and K. V. Morris (2012).  
1030 "Characterization of an HIV-targeted transcriptional gene-silencing RNA in  
1031 primary cells." *Hum Gene Ther* **23**(5): 473-483. DOI: 10.1089/hum.2011.165

- 1032  
1033 Vogt, M., J. Mundig, M. Gruner, S. T. Liffers, B. Verdoodt, J. Hauk, L.  
1034 Steinstraesser, A. Tannapfel and H. Hermeking (2011). "Frequent concomitant  
1035 inactivation of miR-34a and miR-34b/c by CpG methylation in colorectal,  
1036 pancreatic, mammary, ovarian, urothelial, and renal cell carcinomas and soft  
1037 tissue sarcomas." *Virchows Arch* **458**(3): 313-322. DOI: 10.1007/s00428-010-  
1038 1030-5  
1039  
1040 Wang, L., P. Bu, Y. Ai, T. Srinivasan, H. J. Chen, K. Xiang, S. M. Lipkin and X. Shen  
1041 (2016). "A long non-coding RNA targets microRNA miR-34a to regulate colon  
1042 cancer stem cell asymmetric division." *eLife* **5**. DOI: 10.7554/eLife.14620  
1043  
1044 Wang, L., H. J. Park, S. Dasari, S. Wang, J. P. Kocher and W. Li (2013). "CPAT:  
1045 Coding-Potential Assessment Tool using an alignment-free logistic regression  
1046 model." *Nucleic Acids Res* **41**(6): e74. DOI: 10.1093/nar/gkt006  
1047  
1048 Wang, X., J. Li, K. Dong, F. Lin, M. Long, Y. Ouyang, J. Wei, X. Chen, Y. Weng, T. He  
1049 and H. Zhang (2015). "Tumor suppressor miR-34a targets PD-L1 and functions  
1050 as a potential immunotherapeutic target in acute myeloid leukemia." *Cell Signal*  
1051 **27**(3): 443-452. DOI: 10.1016/j.cellsig.2014.12.003  
1052  
1053 Wickham, H. (2016). gtable: Arrange 'Grobs' in Tables. R package version 0.2.0.  
1054 <https://CRAN.R-project.org/package=gtable>  
1055  
1056 Wickham, H. (2017). scales: Scale Functions for Visualization. R package version  
1057 0.5.0. <https://CRAN.R-project.org/package=scales>  
1058  
1059 Wickham, H. (2017). tidyverse: Easily Install and Load the 'Tidyverse'. R package  
1060 version 1.2.1. <https://CRAN.R-project.org/package=tidyverse>  
1061  
1062 Wickham, L. H. a. H. (2017). rlang: Functions for Base Types and Core R and  
1063 'Tidyverse' Features. R package version 0.1.4. [https://CRAN.R-  
1064 project.org/package=rlang](https://CRAN.R-project.org/package=rlang)  
1065  
1066 Wickham, S. M. B. a. H. (2014). magrittr: A Forward-Pipe Operator for R. R  
1067 package version 1.5. <https://CRAN.R-project.org/package=magrittr>  
1068  
1069 Wilkins, D. gggenes: Draw Gene Arrow Maps in 'ggplot2'. R package version  
1070 0.2.0.9003. <https://github.com/wilkox/gggenes>  
1071  
1072 Xiao, N. (2017). liftr: Containerize R Markdown Documents. R package version  
1073 0.7. <https://CRAN.R-project.org/package=liftr>  
1074  
1075 Xie, Y. (2017). knitr: A General-Purpose Package for Dynamic Report Generation  
1076 in R. R package version 1.17. <https://yihui.name/knitr/>  
1077  
1078 Yang, P., Q. J. Li, Y. Feng, Y. Zhang, G. J. Markowitz, S. Ning, Y. Deng, J. Zhao, S.  
1079 Jiang, Y. Yuan, H. Y. Wang, S. Q. Cheng, D. Xie and X. F. Wang (2012). "TGF-beta-  
1080 miR-34a-CCL22 signaling-induced Treg cell recruitment promotes venous

1081 metastases of HBV-positive hepatocellular carcinoma." *Cancer Cell* **22**(3): 291-  
1082 303. DOI: 10.1016/j.ccr.2012.07.023  
1083  
1084 Yap, K. L., S. Li, A. M. Munoz-Cabello, S. Raguz, L. Zeng, S. Mujtaba, J. Gil, M. J.  
1085 Walsh and M. M. Zhou (2010). "Molecular interplay of the noncoding RNA ANRIL  
1086 and methylated histone H3 lysine 27 by polycomb CBX7 in transcriptional  
1087 silencing of INK4a." *Mol Cell* **38**(5): 662-674. DOI: 10.1016/j.molcel.2010.03.021  
1088  
1089 Yu, W., D. Gius, P. Onyango, K. Muldoon-Jacobs, J. Karp, A. P. Feinberg and H. Cui  
1090 (2008). "Epigenetic silencing of tumour suppressor gene p15 by its antisense  
1091 RNA." *Nature* **451**(7175): 202-206. DOI: 10.1038/nature06468  
1092  
1093 Zenz, T., J. Mohr, E. Eldering, A. P. Kater, A. Buhler, D. Kienle, D. Winkler, J. Durig,  
1094 M. H. van Oers, D. Mertens, H. Dohner and S. Stilgenbauer (2009). "miR-34a as  
1095 part of the resistance network in chronic lymphocytic leukemia." *Blood* **113**(16):  
1096 3801-3808. DOI: 10.1182/blood-2008-08-172254  
1097  
1098  
1099  
1100